Deconstructing Best-in-Class Neoglycoclusters as a Tool for Dissecting Key Multivalent Processes in Glycosidase Inhibition

Yan Liang, Rosaria Schettini, Nicolas Kern, Luca Manciocchi, Irene Izzo, Martin Spichty, Anne Bodlenner, Philippe Compain

Chemistry–A European Journal
Research Article
doi.org/10.1002/chem.202304126
Chemistry Europe
European Chemical Societies Publishing
www.chemeurj.org

Deconstructing Best-in-Class Neoglycoclusters as a Tool for Dissecting Key Multivalent Processes in Glycosidase Inhibition

Yan Liang,[a] Rosaria Schettini,[b] Nicolas Kern,[a] Luca Manciocchi,[c] Irene Izzo,[b] Martin Spichty,[c] Anne Bodlenner,*[a] and Philippe Compain*[a]

Multivalency represents an appealing option to modulate selectivity in enzyme inhibition and transform moderate glycosidase inhibitors into highly potent ones. The rational design of multivalent inhibitors is however challenging because global affinity enhancement relies on several interconnected local mechanistic events, whose relative impact is unknown. So far, the largest multivalent effects ever reported for a non-polymeric glycosidase inhibitor have been obtained with cyclopeptoid-based inhibitors of Jack bean α-mannosidase (JBα-man). Here, we report a structure-activity relationship (SAR) study based on the top-down deconstruction of best-in-class multivalent inhibitors. This approach provides a valuable tool to understand the complex interdependent mechanisms underpinning the inhibitory multivalent effect. Combining SAR experiments, binding stoichiometry assessments, thermodynamic modelling and atomistic simulations allowed us to establish the significant contribution of statistical rebinding mechanisms and the importance of several key parameters, including inhitope accessibility, topological restrictions, and electrostatic interactions. Our findings indicate that strong chelate-binding, resulting from the formation of a cross-linked complex between a multivalent inhibitor and two dimeric JBα-man molecules, is not a sufficient condition to reach high levels of affinity enhancements. The deconstruction approach thus offers unique opportunities to better understand multivalent binding and provides important guidelines for the design of potent and selective multiheaded inhibitors.

Introduction

Multivalency has been recognized for more than three decades as a powerful tool used by Nature to achieve strong, yet reversible, binding in situations where monovalent protein-ligand interactions are weak, and hence poorly active.[1] The most prominent examples are found in glycobiology with multisite carbohydrate-binding proteins (lectins).[2] Initially referred to as the "glycoside cluster effect",[3] this phenomenon is involved in essential physiological processes involving protein-carbohydrate recognition events, such as pathogen-cell adhesion, inflammation, fertilization and tumor metastasis.[4] Not surprisingly, multivalency has been applied to therapeutic goals by the synthesis of a myriad of neoglycoclusters.[2,5] These studies have led to the identification of multivalent glycomimetics exhibiting impressive binding enhancements by up to seven orders of magnitude over the corresponding monovalent ligands.[6,7] In the early 2010's, it was shown that multivalent effects approaching those of carbohydrate-lectin interactions could be achieved with multiheaded glycosidase inhibitors.[8] These somewhat counterintuitive results triggered a wave of interest into the potential of multivalent design for modulating glycosidase activity.[9] Huge efforts were made to rationalize a phenomenon that was difficult to comprehend based on the mechanistic paradigms developed so far in multivalency studies.[2] No large multivalent effect was indeed expected to occur with glycosidases. In contrast to lectins displaying multiple carbohydrate recognition domains (CRDs), enzymes typically possess only one substrate binding site. The bridging of several CRDs by multivalent ligands, a mode of binding termed as the chelate effect, is thus theoretically not possible.[10] This point is crucial considering that chelation mechanisms account for the largest multivalent effects reported so far.[6,7,10] Over more than a decade, a diversity of studies has been performed to address the puzzling question of how reversible multivalent inhibitors and glycosidases interact to produce high binding enhancements. Most of them rely on the synthesis of libraries of neoglycoclusters bearing multiple copies of inhibiting epitopes (inhitopes) and on the use of physical methods including

[a] Dr. Y. Liang, Dr. N. Kern, Dr. A. Bodlenner, Prof. P. Compain
Laboratoire d'Innovation Moléculaire et Applications (LIMA), University of Strasbourg | University of Haute-Alsace | CNRS (UMR 7042), Equipe de Synthèse Organique et Molécules Bioactives (SYBIO), ECPM, 25 Rue Becquerel, 67087 Strasbourg (France).
E-mail: philippe.compain@unistra.fr
annebod@unistra.fr

[b] Dr. R. Schettini, Prof. I. Izzo
Dipartimento di Chimica e Biologia "A. Zambelli", Università degli Studi di Salerno, 84084 Fisciano (Salerno), Italy

[c] L. Manciocchi, Dr. M. Spichty
Laboratoire d'Innovation Moléculaire et Applications (LIMA), University of Strasbourg | University of Haute-Alsace | CNRS (UMR 7042)–IRJBD, 3 bis rue Alfred Werner, 68057 Mulhouse Cedex (France)

Supporting information for this article is available on the WWW under https://doi.org/10.1002/chem.202304126

isothermal titration calorimetry (ITC) or atomic force microscopy (AFM).[9] The focus has been made on Jack bean α-mannosidase (JBα-man), a member of the clinically relevant glycoside hydrolase family 38 (GH38).[11] More than ten years after the discovery of the first large inhibitory multivalent effects,[8,12] this dimeric high-molecular-weight glycosidase is still the most sensitive to multivalent presentation of inhitopes known to date. In this context, and after extensive structure-activity relationship (SAR) studies, our team identified **1**, a 36-valent cyclopeptoid-based iminosugar showing the largest multivalent effect ever observed for a non-polymeric glycosidase inhibitor with a relative inhibition potency per inhitope unit (*rp*/*n*) close to 5000-fold with respect to the monovalent reference **2** (Figure 1A).[13,14] The reversible formation of a 2:1 JBα-man-glycocluster complex was first suggested based on mechanistic studies using three different techniques, including electron microscopy imaging (EM) and ultracentrifugation sedimentation velocity (AUC-SV) (Figure 1B).[13] This result was unambiguously confirmed few years later by the high resolution crystal structure of JBα-man complexed with the 36-valent cluster **1** in which four 1-deoxynojirimycin (DNJ) inhitopes simultaneously engage all four active sites of two dimeric JBα-man molecules.[15] The formation of a sandwich-type cross-linked complex is likely to produce a strong chelate effect involving 2x2-binding sites (Figure 1B). In addition to chelation mechanisms, clustering binding modes, i.e. simultaneous binding by a multivalent ligand of CRDs of more than one protein, are also at play (Figure 1C). This would explain the exceptionally high binding enhancements observed. However, the accuracy of our interpretation model is questionable considering the fact that multivalent binding is based on a complex supramolecular network of other interactions having enthalpic and entropic contributions that may work in concert (Figure 1C).[2] Occlusion of the active site by large glycoclusters can, for example, hamper the approach of natural substrates via non-specific interactions with aglycone/non-glycone subsites ("recognition and blockage" mechanism).[9] Statistical rebinding effects leading to reduced off-rates may be also promoted by high local concentration of the dissociated inhitopes. It is widely accepted as a general principle, if not dogma, that non-chelation effects are weaker multivalent interaction mechanisms where chelation binding is operative.[10,16] However, very few studies in the field of protein-carbohydrate interactions have been devoted so far to dissecting the relative contributions of chelation, statistical rebinding and other effects.[16–18] Multivalent binding data were extracted from Surface Plasmon Resonance (SPR) kinetic analysis[16] or more classical SAR approaches.[17,18] Needless to say, such efforts are hampered by the complexity of the interconnected local mechanistic events at play. In the context of multiheaded glycosidase inhibitors, we were convinced that the identification of neoglycocluster **1**–the current "gold standard"–provides a unique opportunity for attempts to better understand the complex, interconnected mechanistic events underlying high multivalent effects. In contrast to most SAR studies which typically aim to select and optimize the best hits, our strategy is based on the top-down deconstruction of the

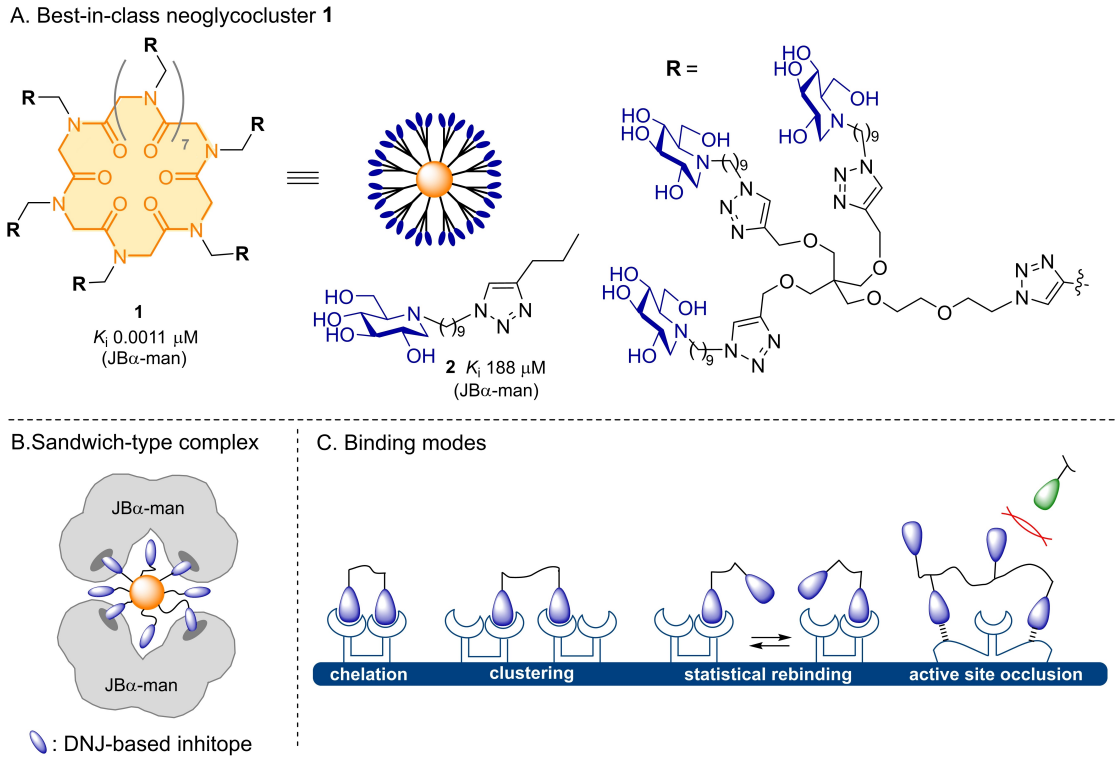

Figure 1. Multivalent interactions of JBα-man with DNJ cluster **1**. A) Structure of **1** and its inhibition potency against JBα-man. B) Schematic representation of JBα-man protein structure in complex with 36-valent cluster **1**. C) Theoretical multivalent binding modes between multimeric protein receptor(s) and a simplified multivalent ligand.

prevailing, best-in-class lead compound. Reverse thinking and deconstruction approaches may provide powerful, yet counter-intuitive tools to apprehend complexity as beautifully illustrated in the field of total synthesis by E. J. Corey with the retrosynthetic analysis concept.[19]

Here, we present the full details of our deconstruction approach from the design, synthesis and evaluation of tailored multivalent inhibitors to the determination of the binding stoichiometry using AUC-SV. In combination with thermodynamic modelling and atomistic simulations, our study sheds new lights on the complex mechanisms underpinning multivalent effect in enzyme inhibition.

Results and Discussion

Design

Results from previous SAR studies combined with crystallographic analysis have clearly shown that the key constituents – scaffold, linker, inhitope – of neoglycocluster **1** meet the adequate structural requirements in terms of size and geometry to reach high multivalent effects and form a sandwich-type cross-linked complex with two dimeric JBα-man molecules. Following a deconstruction approach, a new series of multivalent cyclopeptoid-DNJ conjugates **3**–**7** were synthesized from cyclopeptoid scaffolds **8**–**12** and DNJ-linker conjugates **13**–**15** (Figures 2–4). These lower valency clusters were designed to be structurally as close as possible to the best-in-class compound **1**; clusters **1** and **3**–**7** have the same scaffold size and linker length as shown in Figure 2. The convergent synthesis of glycodendrimer **1** was based on the grafting of azide-armed trivalent DNJ dendron **13** to the "clickable" alkyne-functionalized cyclopeptoid scaffold **12** (Figures 3–4).[13] We first envisaged the synthesis of different types of 12-valent analogues in which the tripodal moieties are totally, partially, or not conserved at all. Formal removal of two inhitopes out of the three carried by each dendron leads to cluster **3**, the closest analogue of **1**. To mimic the missing aliphatic spacers, the *N*-nonyl DNJ moieties were replaced by tetraethyleneglycol arms to maintain solubility in water and similar steric bulk. Full removal of the corresponding dendritic arms gave cluster **4** having 12 DNJ units (Figure 2). The synthesis of DNJ clusters **5a**–**c** exhibiting local inhitope density similar to the one of **1** served to complete the series of 12-valent clusters. These compounds were prepared from three different functionalized

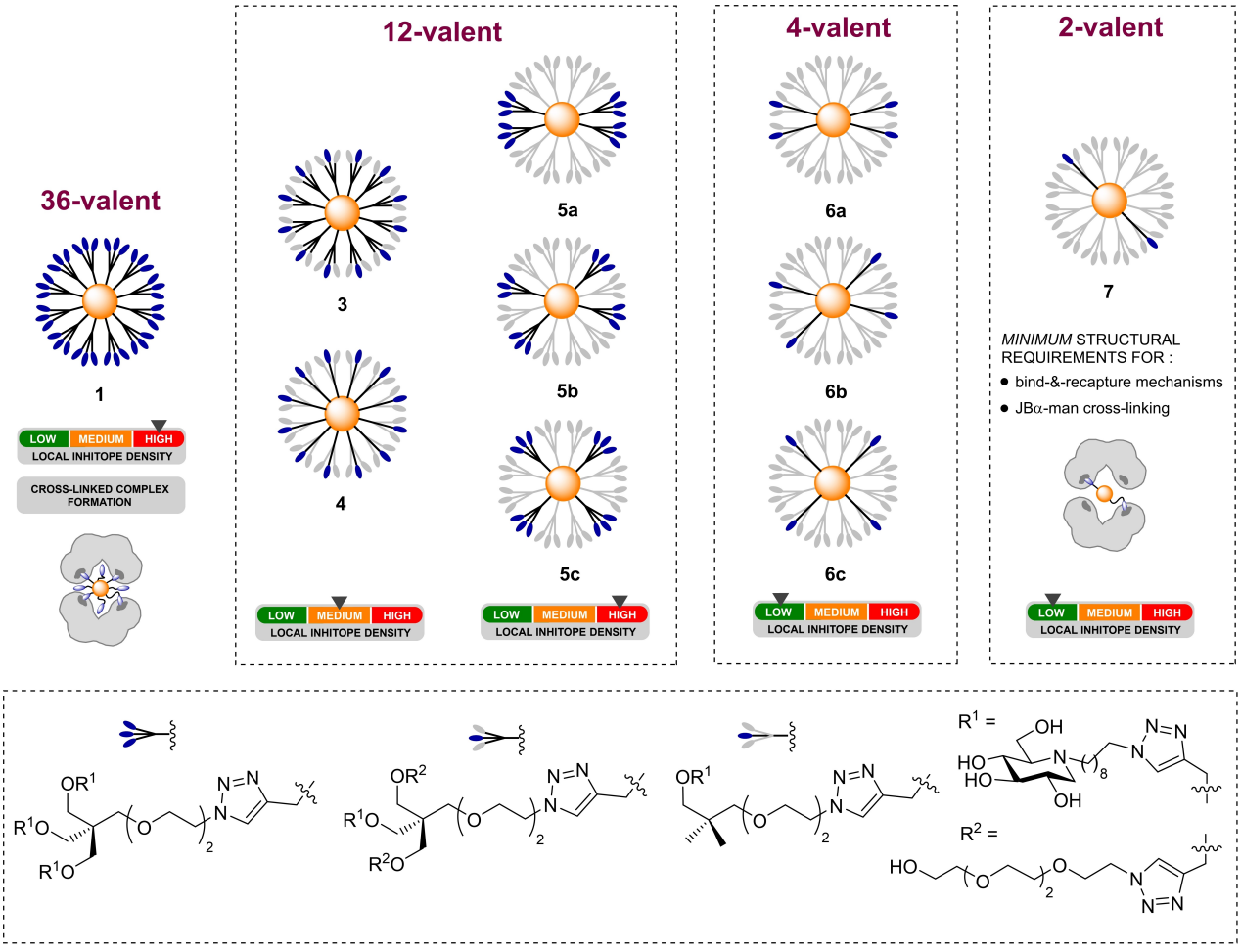

Figure 2. Design of cyclopeptoid-based DNJ clusters **3**–**7** (for the representations of the complete structures of **1**, **4** and **5c**, see Figures S2–4).

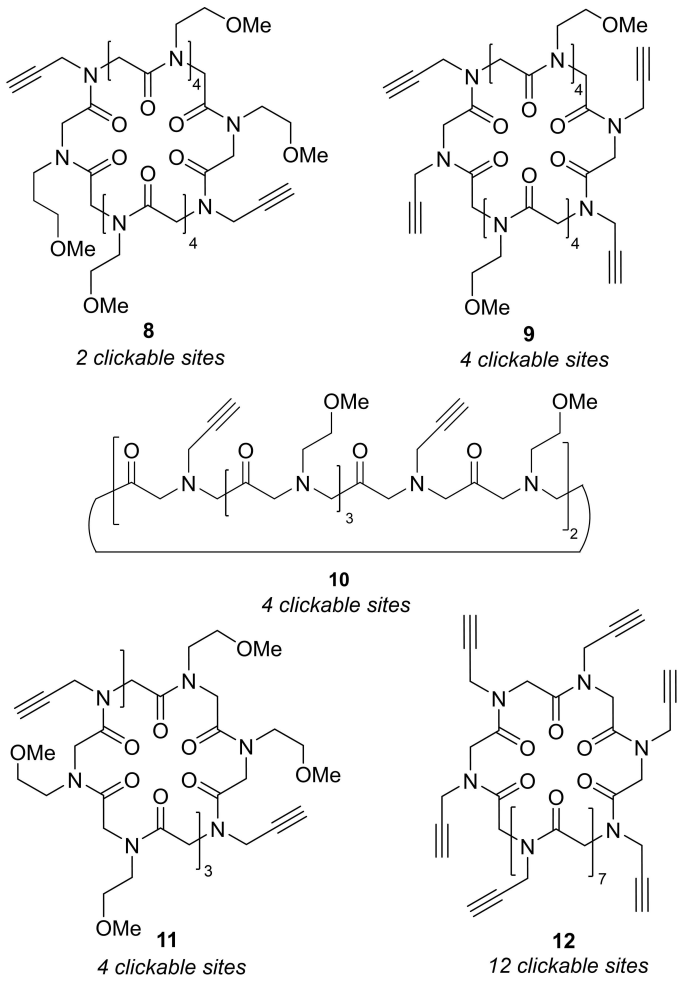

Figure 3. Propargylated "clickable" scaffolds **8**–**12**.

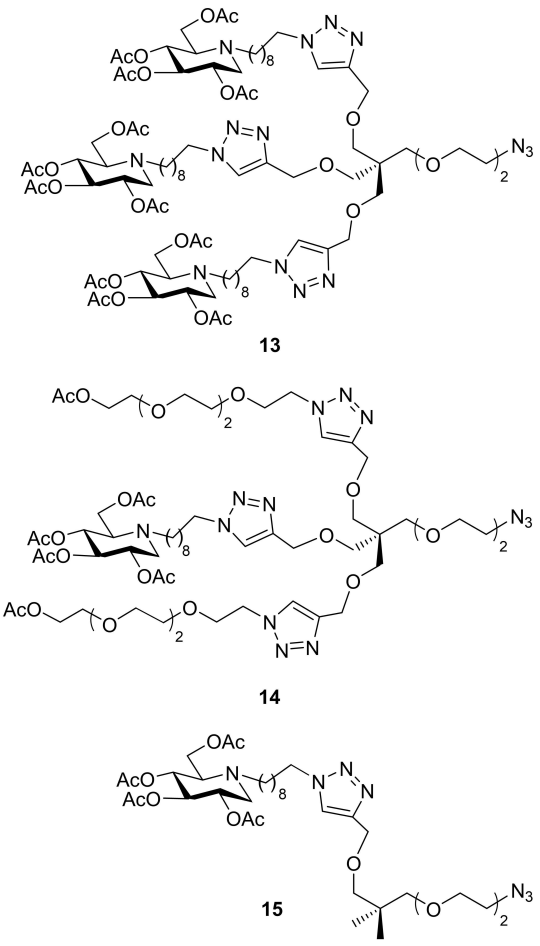

Figure 4. Azide-armed ligands **13**–**15**.

scaffolds – compounds **9**–**11**–which differ by the position of the four clickable terminal alkyne functions on the cyclopeptoid core (Figure 3). These tetravalent scaffolds were also used to synthesize 4-valent clusters **6a**–**c** bearing the same linear DNJ-containing arm as in the 12-valent inhibitor **4**. Finally, divalent DNJ **7** with diametrically opposed inhitopes was envisioned as the most extreme compound of the whole series. Tetravalent clusters **6** and the corresponding divalent analogue **7** have theoretically the minimum structural requirement to cross-link two JBα-man molecules, with active sites being occupied by four and two inhitopes, respectively.

Synthesis

To synthesize the new neoglycoclusters **3**–**7**, we logically applied the same modular strategy as the one used for the preparation of 36-valent cluster **1**.[13] This convergent approach required the grafting of azide armed trivalent dendron **13** or related mono-headed analogues **14**–**15** onto alkyne-functionalized cores **8**–**12** composed of 12 *N*-alkylated glycine units (Figures 3–4, Schemes 1–3).[20] Akin to best-in-class inhibitor **1**, highly symmetrical 12-valent DNJ clusters **3** and **4** were constructed from the polyalkyne scaffold **12**.[13] The preparation of cyclopeptoid scaffold bearing two or four clickable terminal alkyne functions was achieved by the replacement of *N*-propargylated glycines with *N*-methoxyethyl glycines by taking advantage of the sub-monomer solid-phase approach developed by Zuckermann *et al.*[20a] For 12-valent clusters **5**, three

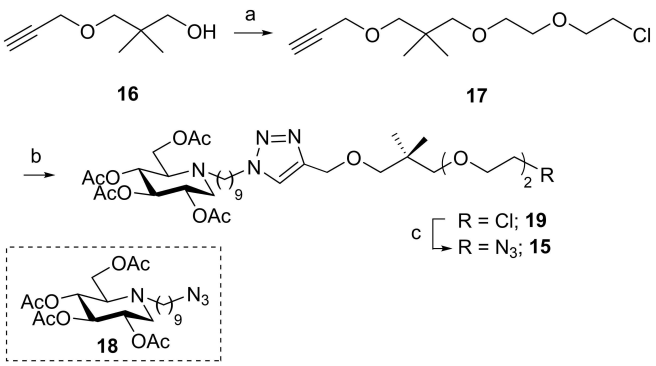

Scheme 1. *Reagents and conditions*: Synthesis of DNJ-linker conjugate **15**: (a) 1-Chloro-2-(2-chloroethoxy)ethane, 50% aq. NaOH, *n*-Bu_4NHSO_4, 35 °C (62%); (b) **18**, $CuSO_4 \cdot 5H_2O$ cat., sodium ascorbate, DMF/H_2O, MW, 80 °C (98%); (c) *n*-Bu_4NI, NaN_3, DMF, 80 °C (95%).

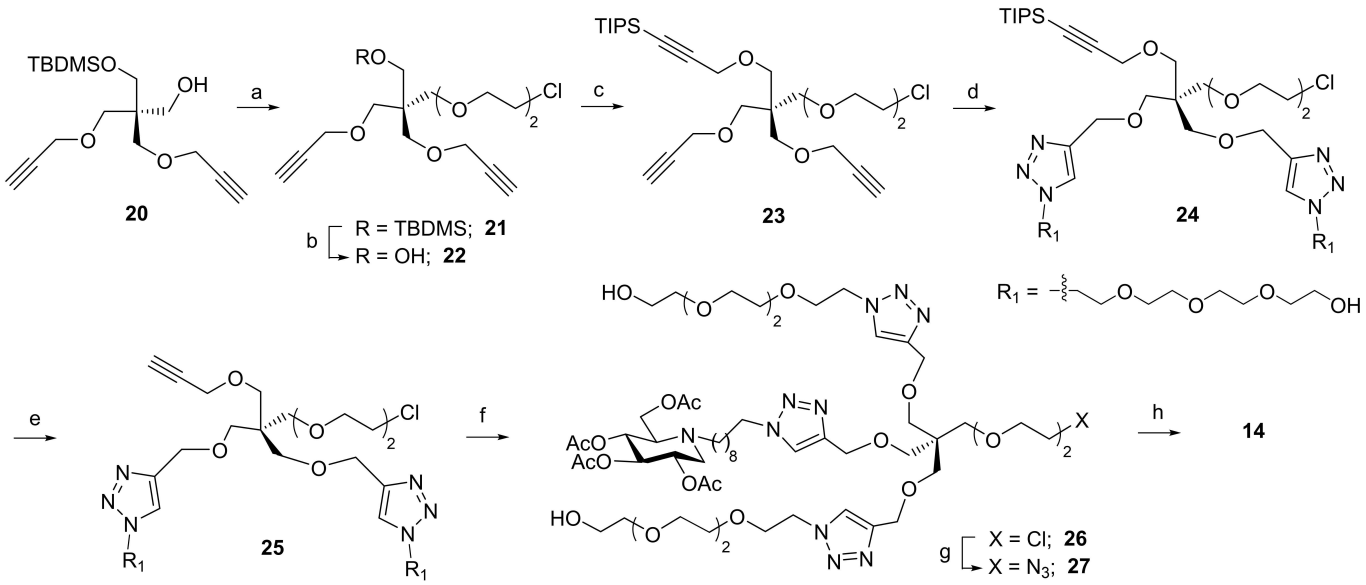

Scheme 2. *Reagents and conditions*: Synthesis of DNJ-linker conjugate **14**: (a) NaH, $Cl(CH_2)_2O(CH_2)_2OTf$, THF, 0 °C (78%); (b) *n*-Bu_4NF, THF, 0 °C to rt (97%); (c) 3-Bromo-1-(triisopropylsilyl)-1-propyne, NaH, THF, 0 °C to rt (67%); (d) Tetraethylene glycol azide, $CuSO_4 \cdot 5H_2O$ cat., sodium ascorbate, DMF/H_2O, MW, 80 °C (97%); (e) AgF, MeCN, rt, then HCl 1 M, rt (85%); (f) **18**, $CuSO_4 \cdot 5H_2O$ cat., sodium ascorbate, DMF/H_2O, MW, 80 °C (96%); (g) NaN_3, *n*-Bu_4NI cat., DMF, 80 °C (92%); (h) Ac_2O, Py, rt (98%).

different scaffolds (**9**–**11**) in which the distance between the iminosugar-based dendrons differed were synthesized.

In **5a**, the DNJ-containing tripods were grafted on adjacent glycine units, whereas in **5b** and **5c** they were separated by one and two glycine units, respectively. Compounds **9**–**11** are already described together with their single crystal X-ray structures.[20b] The same scaffolds **9**–**11** were used for the synthesis of the three 4-valent clusters **6a**–**c**. Dimer **7** bearing diametrically opposed DNJ heads was prepared from scaffold **8** (Figure 3).[20c]

Inhitope-linker conjugate **15** was prepared from the key building block *N*-nonyl DNJ azide **18** (Scheme 1).[21]

Known monopropargylated **16**[22] was alkylated by 1-chloro-2-(2-chloroethoxy) ethane to provide alkyne **17**. Copper (I)-catalyzed azide alkyne cycloaddition (CuAAC) reaction between *N*-nonyl DNJ azide **18** and chloroalkyne **17** yielded almost quantitatively chloride **19**, which was then substituted by sodium azide to give azide-armed inhitope-linker conjugate **15**. Preparation of ligand **14** relied on sequential functionalization of selectively protected pentaerythritol (Scheme 2). The key intermediate of this synthesis was dipropargylated alcohol **20**, which can be obtained thanks to a partial propargylation of monosilylated pentaerythritol.[23] Alkylation of the neopentylic alcohol **20** failed with 2,2′-dichlorodiethylether, but could be achieved with 2-(2-chloroethoxy)ethyl triflate[24] in 78% yield.

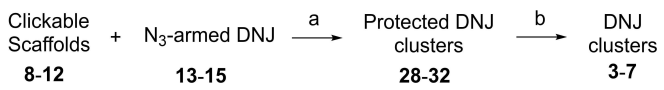

Scheme 3. *Reagents and conditions:* Synthesis of neoglycoclusters **3**–**7**: (a) $CuSO_4 \cdot 5H_2O$ cat., sodium ascorbate, DMF/H_2O, MW, 80 °C; (b) IRA-400 (OH^-), MeOH/H_2O (1:1), rt (yields are given in Table 1).

TBS removal using TBAF was followed by alkylation with TIPS-protected propargyl bromide.[25–26] First, tetraethylene glycol azide[27] was grafted on dialkyne **23** by CuAAC in 97% yield. Silver fluoride-promoted deprotection of TIPS-alkyne **24** yielded **25** which was engaged in a second CuAAC step with *N*-nonyl DNJ azide **18** to give **26** in 85% yield. Chloride to azide substitution afforded the DNJ-linker conjugate **27**. CuAAC reactions are known to proceed well in the presence of many functional groups, including alcohols.[28,8] However, the CuAAC reaction between **27** and scaffold **12** failed to give the desired corresponding DNJ cluster. This unexpected result led us to protect diol **27** to give the clickable mono-headed inhibitor **14**. The small library of clusters **3**–**7** was eventually obtained in two steps by tactical CuAAC coupling between azide-armed inhitopes **13**–**15** and cyclopeptoid scaffolds **8**–**12** followed by *O*-deacetylation using an amberlite IRA-400 (OH^-) (Scheme 3 and Table 1).

Enzymatic Evaluation

The new series of DNJ clusters **3**–**7** was evaluated in triplicate as JBα-man inhibitors (Table 2). In line with the results obtained with 36-valent cluster **1**,[13] all display competitive inhibition (Figures S5–S15). Of note, for 12 valent inhibitors **4**–**5**, when the secondary curve of Lineweaver-Burk plot was not linear, we used a nonlinear fit with Morrison equation[29,30] for competitive inhibitors considering the enzyme concentration.[23]

We first evaluated highly symmetrical 12-valent DNJ **3** and **4** as the closest analogues of best-in-class cluster **1**. The formal removal of two *N*-nonyl DNJ units per dendron resulted in a dramatic reduction of the inhibitory multivalent effect with a relative inhibition potency per inhitope unit (*rp*/*n*) reduced by

Table 1. Neoglycoclusters **3**–**7** synthesized from cyclopeptoid scaffolds **8**–**12** and DNJ-linker conjugates **13**–**15**.

Scaffold	DNJ-Linker	Protected Cluster	Cluster	Valency	Yields[a]
12	**14**	**28**	**3**	12 (12×1)	53%
12	**15**	**29**	**4**	12 (12×1)	68%
9	**13**	**30a**	**5a**	12 (4×3)	79%
10	**13**	**30b**	**5b**	12 (4×3)	63%
11	**13**	**30c**	**5c**	12 (4×3)	49%
9	**15**	**31a**	**6a**	4	82%
10	**15**	**31b**	**6b**	4	63%
11	**15**	**31c**	**6c**	4	72%
8	**15**	**32**	**7**	2	64%

[a] Isolated yields (2 steps).

one order of magnitude compared to **1**. The strongest effect was observed for cluster **3** with a *rp*/*n* value reduced by a factor of 20. Formal removal of PEG arms in **3** to give **4** led to a better relative inhibition potency (370-fold *vs.* 210-fold on a valency-corrected basis). This may suggest that the PEGylated linkers have a detrimental effect on the DNJ heads accessibility or solvation (see below). 12-Valent glycodendrimers **5a**–**c** with a higher local inhitope density were then evaluated. Interestingly, they were found to display similar multivalent effect compared to **3** with *rp*/*n* values up to 190-fold. No significant difference in inhibition was observed between glycodendrimers **5a**, **5b** and **5c**. The impact of the position of the tripod units on the cyclopeptoid core is likely to be counterbalanced by the flexibility and the length of the nonyl and PEG linkers. A similar effect was observed with 4-valent clusters **6a**–**c** which showed comparable K_i values of 2–3 μM. The formal replacement of trivalent dendrons in **5** by the corresponding mono-headed units to give 4-valent DNJ **6** reduces the multivalent effect by one magnitude order as judged by *rp*/*n* values. Remarkably, the same cause produces the same quantifiable effect: from 36-valent cluster **1** to 12-valent cluster **4**, as shown above, the *rp*/*n* value is also reduced by one order of magnitude. This result also highlights one of the interests of the deconstruction approach. The impact of a given structural modification – the diminution of the local inhitope density – could be evaluated twice, *ceteris paribus* (all else being equal), and the results obtained confirmed at least once. Finally, the smallest divalent cluster **7** displayed a small, but quantifiable multivalent effect ($rp/n > 1$), being threefold more active than the monovalent reference **2**.

Stoichiometry Assessment by Analytical Ultracentrifugation

A first important step towards the rationalization of the inhibition results required the evaluation of the stoichiometry of the complexes between JBα-man and clusters **3**–**7**. Analytical ultracentrifugation sedimentation velocity (AUC-SV)[31–34] was selected as the tool of choice with regards to binding stoichiometry determination. In this technique, there is no

Table 2. Relative inhibition potencies of DNJ clusters **3**–**7**, inhibitory activity (K_i, μM) against JBα-man and binding stoichiometry from AUC-SV.

Cluster	Valency	K_i (μM)	*rp*[a]	*rp*/*n*[b]	$\frac{rp}{n(n-1)}$[c]	BS[d]
2	1	188[21]	–	–	–	–
1	36	0.0011[13]	170,000	4,700	134	2:1
3	12 (12×1)	0.074	2500	210	19	1:1
4	12 (12×1)	0.042	4500	370	34	2:1
5a	12 (4×3)	0.084	2200	190	17	1:1
5b	12 (4×3)	0.12	1600	130	12	1:1
5c	12 (4×3)	0.097	1900	160	15	1:1
6a	4	3.1	61	15	5.1	1:1
6b	4	2.2	85	21	7.1	1:1
6c	4	2.3	82	20	6.8	1:1
7	2	54	3.5	1.7	1.7	1:1

[a] Relative inhibition potency ($rp = K_i$ (monovalent reference **2**)/K_i(cluster)). [b] *rp*/*n* = *rp*/*number of DNJ units.* [c] Evaluation of a possible proportionality relationship between *rp* and *n(n-1)* (See theoretical part for more details). [d] BS=Binding Stoichiometry of the major $(LH)_2$/cluster complex species present in solution as determined by AUC-SV experiments (for more information, see Figure S16 and Table S1).

interaction with a stationary phase and no change in the sample composition, as for size-exclusion chromatography (SEC) or field-flow fractionation (FFF).[35] Clusters **3**–**7** required DMSO to make stock solutions. This requirement is compatible with AUC-SV, providing that the small percentage of DMSO is the same for all samples. In contrast, the use of DMSO is unfavorable for ITC, because DMSO dilution heats are very large, leading to poorly reliable results.[36] In solution, JBα-man alone is a well-defined enzyme composed of two LH heterodimers $(LH)_2$ with an average sedimentation coefficient of 9.3S corresponding to an estimated MW of 218 kDa, accompanied by 8% of 2×$(LH)_2$, the complex of two enzymes (Figures S16 and table S1 in the Supporting Information).[13] All samples were analyzed for three sedimentation ranges: the one corresponding to the size of one enzyme (8.45S to 11S), the one corresponding to aggregates of two enzymes (13S to 16.6S) and an intermediate range (11S to 13S), related to the dynamic equilibrium between the two main complexes.[33] The AUC–SV results indicated that most of the DNJ clusters are associated with the enzyme in a 1:1 fashion (Table 2). The only exception is found with 12-valent cluster **4** which forms a sandwich-type 2:1 complex with JBα-man as the best-in-class cluster **1**. Surprisingly, despite its close structural analogy with clusters **1** and **4**, 12-valent DNJ **3** is not able to cross-link two JBα-man molecules. As shown also with DNJ-cyclopeptoid conjugates **5** and **6**, fulfilment of the appropriate structural requirements is not a sufficient condition to generate a sandwich-type complex with two dimeric JBα-man molecules, even when the local inhitope density is high (glycodendrimers **5**). How to explain that 12-valent cluster **4** demonstrates the ability to cross-link two dimeric enzymes while its closely related analogues **5** do not? The main difference between these clusters is that **4** is closer to afford a radial presentation of inhitopes, without any topological restriction, each DNJ head being equally accessible to each active site, at least considering the fully elongated conformer (see below). Comparison of *rp*/*n* values and binding stoichiometry provides interesting insights into the mechanisms underlying the inhibitory multivalent effect. Divalent DNJ **7**, the simplest member of the DNJ cluster series, was designed to minimize statistical rebinding mechanisms while still allowing the cross-linking of two different enzymes (Figure 2). In the absence of a sandwich-type 2:1 complex as evidenced by AUC–SV, the small but quantifiable multivalent effect (*rp*/*n* 1.7) is likely to be almost uniquely attributed to statistical rebinding effects. Key observations were obtained from 12-valent clusters **3**, **4** and **5** which display similar range inhibition values (Table 2). Strong chelation effects provided by the formation of a cross-linked complex between JBα-man and **4** led to the better inhibition values of the new series of clusters **3**–**7**, but were not sufficient to provide a sharp difference in affinity gain among the 12-valent clusters series (compound **4** *versus* **3** and **5**). In contrast, the deconstruction study highlights the importance of statistical rebinding with a one magnitude order gain between 4-valent DNJ **6a**–**c** and 12-valent DNJ **5a**–**c**, as well as between **4** and **1**, that is to say between clusters sharing the same functionalized scaffold but with a different local inhitope density (three close DNJ heads *versus* one). The same gain is thus observed whether the clusters are able to generate a cross-linked complex with two JBα-man molecules (**4** and **1**) or not (**6** and **5**). Interestingly, in their study of the binding of lectin DC-SIGN with semi-rigid rod-based dendrimers terminated with two trivalent dendrons, Bernardi, Fieschi *et al.* also found a gain of one order of magnitude when chelation mechanism became attainable, and of two orders of magnitude when statistical rebinding effects cumulated with chelation.[18] In the present study, the *rp*/*n* values were decreased by two orders of magnitude from 36-valent DNJ **1** to the corresponding 4-valent DNJ analogues **6**.

Theoretical considerations and molecular modelling

To further elucidate the factors influencing the multivalent effect of the studied clusters, we tested an existing well-known thermodynamic model on our data and performed atomistic simulations to encompass the validity of this model. For the sake of readability and conciseness, only the essence of the theoretical results is highlighted here. The reader is referred to the companion article for complete details.[37] Thermodynamic modeling can indeed help to understand the basis of multivalency effects. Kitov and Bundle determined thermodynamic models for the inhibition of multisite receptors by multivalent ligands.[38] These models were developed for various receptor: ligand topologies and under the assumption of 1:1 stoichiometry. The radial topology appears as the most adequate for our case: the *n* branches of the ligand (clusters **1** and **3**–**7**, $n = 2$–36) are centrally anchored so that each DNJ head can interact independently and identically strong with the *m* binding sites of the receptor (JBα-man, $m = 2$). Under these conditions, the equilibrium constant for the formation of the fully inhibited receptor K_{eq} ($\propto 1/K_i$) is given by:

$$K_{eq} = \gamma\, n(n-1) \propto rp \text{ for } n \geq 2 \quad (1)$$

where γ is a proportionality constant valid for all cluster ligands. Accordingly, K_{eq} is expected to display a n^2-like dependency for large values of *n*. The companion article[37] provides an alternative derivation of Eq. 1 based on macroscopic rate constants and shows also that K_{eq} is proportional to the relative inhibition potency *rp*. Kitov and Bundle applied statistical thermodynamics to show that the factor $n(n–1)$ in Eq. 1 results from the degeneracy coefficient Ω when radial topology is assumed. Ω accounts for the fact that the fully inhibited receptor is not "an individual molecule but an ensemble of Ω microscopically distinguishable complexes."[38] In our case, the degeneracy factor measures the number of possible combinations to form a complex between a receptor with two binding sites and a ligand with *n* identical and independent inhitopes. Before testing the experimental *rp* values with Eq. 1, we wanted to probe the assumption of radial topology for the studied clusters. Therefore, we investigated the geometric properties for a subset of different clusters with the aid of full-atom molecular mechanics. We determined the distribution of intramolecular DNJ-DNJ distances for clusters **1** ($n = 36$), **6c** ($n = 4$)

and **3**, **4**, **5c** ($n=12$) (Figure 5A). Ideal radial topology would imply that the distributions of distances are identical for all clusters when normalized by $n(n-1)$. As shown in Figure 5C, the distributions are indeed rather similar. The distributions become slightly broader with increasing valency. As a result, the probability of finding two inhitopes at a distance of ca. 35 Å (= separation of binding sites in the monomeric enzyme, yellow bar in Figures 5B and 5 C) increases with valency. On the other hand, the solvent accessibility of the inhitopes (Figure 5D) slightly decreases with valency. In general, it can be expected that these two compensatory trends are expected to cancel out (to some extent). There are, however, some particularities. For example, glycoclusters **3** and **4** (both $n=12$) display rather similar normalized distributions of DNJ-DNJ distances. The accessibility of the sugar heads is, however, very different (see Figure 5D). Cluster **3** features 12 tripod branches, each with two ghost side-arms, i.e., arms that are not decorated by a DNJ inhitope. These ghost side-arms shield the remaining inhitope-decorated arm from the solvent (Figure 5E). In glycocluster **4** with 12 unipod branches these ghost-arms are not present and the accessibility of the inhitopes is substantially increased with respect to cluster **3**. This could explain a higher chemical activity of the DNJ heads and therefore a higher inhibition potency of **4** with respect to **3**.

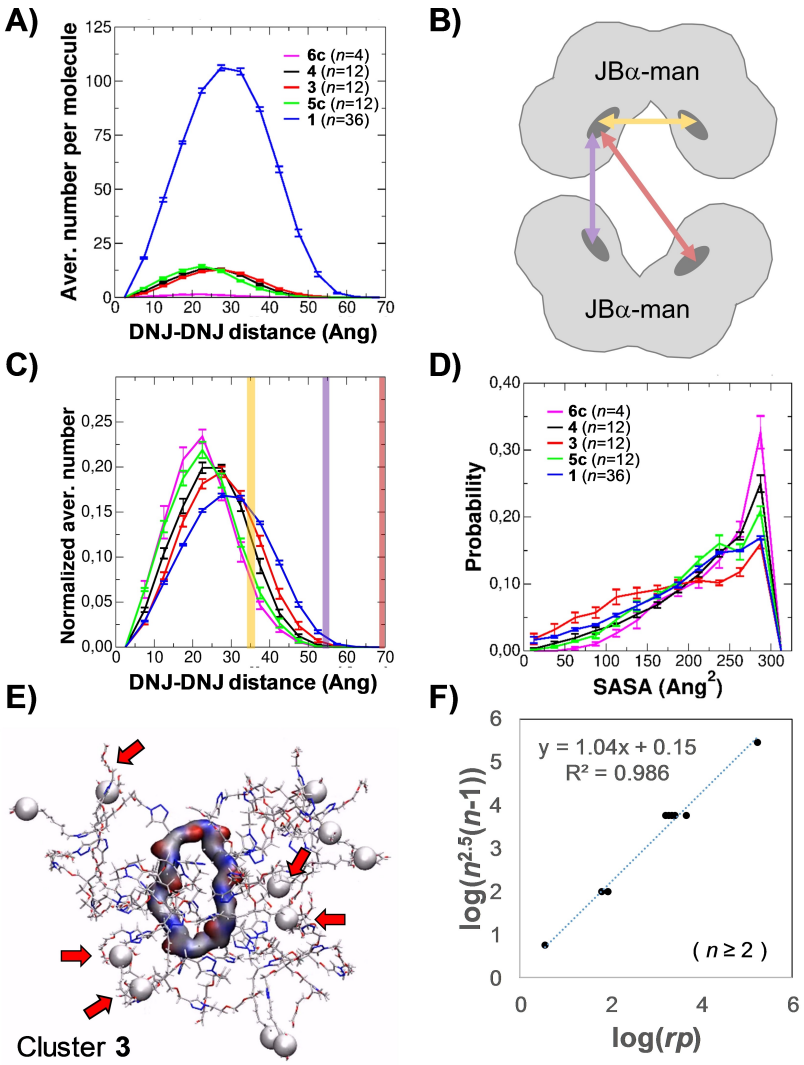

Figure 5. A) Distribution of intramolecular DNJ-DNJ distances as determined from four molecular dynamics simulations in explicit water (TIP3P); each simulation started from a different structure as obtained from simulated annealing with an implicit solvation model.[37] The total length of each simulation was 300 ns; the first 100 ns served for equilibration. Error bars correspond to standard error of the mean when averaging over the four independent simulations. All sugar heads featured the same protonated state to be in line with the conditions of radial topology. The nitrogen atom of the DNJ head was used to calculate the distance between the sugar heads. According to the Gauss formula there are in total $nx(n\text{-}1)/2$ such distances, i.e., 36x35/2, 12x11/2 and 4x3/2 for $n=36$, $n=12$, and $n=4$, respectively. B) Schematic representation of the crystal structure of the JBα-man dimer with complexed cluster **1** (PDB entry: 6B9B).[15] C) Same as A) but with a normalization factor $n(n\text{-}1)$ applied. The bars indicate the distances between the four receptor binding sites as shown in B). D) Probability of finding an DNJ head with a given solvent accessible surface (SASA). The probability distribution was obtained by binning the SASA values of all heads and all MD snapshots. E) A typical snapshot from the MD simulation of 12-valent glycocluster **3**. The white spheres indicate the position of the nitrogen atoms of the DNJ heads. The backbone bonds are shown as thick tube; the remaining bonds as thin sticks. The arrows indicate ghost arms shielding 5 of 12 DNJ heads. F) Log-log plot of the relative inhibition potency (rp) and the empirically found n-dependency $n^{2.5}(n-1)$. The optimal power of n was obtained by varying it from 2 to 4 in steps of 0.5; the power of 2.5 yielded the slope closest to unity (1.04) for the regression line (dashed line).

Another particularity concerns the 12-valent glycoclusters **5a–c** that feature a tripod branch type with three inhitope-decorated arms. Obviously, inhitopes from the same branch cannot simultaneously bind at two different sites of the receptor (that are too far away). Or, in other words, inhitopes from the same branch (*tripod* case) are closer to each other than inhitopes from different branches. This is also seen by a shift of the normalized distribution of sugar-sugar distances to lower values (i.e., shift to the left in Figure 5C) when comparing **5c** with the *unipod* cluster **4**; the latter does not suffer from such geometric constraints. Thus, the degeneracy coefficient of **5a–c** is only 12×9 = 108 and therefore reduced with respect to **4** (12×11 = 132). This is reflected by a reduced inhibition potency. Obviously, cluster **1** suffers also from these geometric constraints but the influence on the degeneracy coefficient is much less pronounced in relative terms.[37] While radial topology seems in principle valid for all studied clusters from a structural point of view (with some minor deviations as discussed above), we note that Eq. 1 does not capture the full extent of the multivalency effect (Table 2, penultimate column): *rp* is not proportional to $n(n-1)$ but we find empirically:

$$rp \propto n^{2.5}(n-1) \text{ for } n \geq 2 \quad (2)$$

(see Figure 5F).

Thus, *rp* displays a $n^{3.5}$-like dependency for large values of *n*. To our understanding there are two potential explanations (or a combination of both) for this behavior:

1) *Possibility to form complexes with 2:1 stoichiometry* (2 JBα-man receptors:1 multivalent inhibitor). These complexes feature four receptor binding sites which leads to higher order terms, i.e., additional n^3- and n^4-terms, to properly describe the degeneracy coefficient.[38] If 2:1 complexes were responsible for the $n^{3.5}$-like dependency of *rp*, it would imply that the fraction of formed 2:1 complexes should increase with the valency.[38] Indeed, high-valency glycoclusters **1** and **4** are the only clusters of the series that have been found to form 2:1 complexes and share similar amount of those complexes whereas their valency are respectively 36 and 12. It also remains an open question why **4** is the only 12-valent cluster than can form 2:1 complexes. Glycocluster **3** probably features a too low DNJ head accessibility while clusters **5a–c** suffer from too many geometric constraints (too low degeneracy coefficient Ω), both factors being of course of relevance to form 2:1 complexes.[37,38]
2) *Increasing favorable electrostatic interactions with increasing inhitope valency.* At pH = 5.5, the *apo* receptor JBα-man features an overall negative charge of about −6.6*e* as obtained from continuous constant-pH molecular dynamics simulations.[37] The inhitopes, however, are charged positively. For example, **6c** ($n = 4$) and **5c** ($n = 12$) are charged +2.4*e* and +5.4*e*, respectively, due to the partial protonation of the iminosugars. It is well known that electrostatics play a crucial role for the associations of macromolecules.[39] By including electrostatics for oppositely charged macromolecules in polar solvents (such as water), it is rather straightforward to derive an expression similar to Eq. 2 (as observed by the experiments).[37] This electrostatic contribution to the multivalent effect is supposed to be pH-dependent: the total charge of the receptor changes its sign from −6.6*e* at pH = 5.5 to +9.4*e* at pH = 4.0 (the isoelectric point of this receptor is at about pH = 5). Thus, at pH = 4 repulsive electrostatic interactions are expected between the positively charged receptor and the positively charged ligand (in contrast to attractive interactions at pH = 5.5). And this repulsion would increase with increasing inhitope valency, i.e., with increasing positive charge of the DNJ heads. To test this hypothesis, inhibition constants of two representative compounds have been measured at pH = 4. The enzyme activity was unaffected at that pH and the inhibition constant of the 4-valent cluster **6c** increases from 2.3 μM (at pH = 5.5) to 184 μM (at pH = 4), which correspond to a decrease in inhibition potency of about 80-fold. The inhibition constant of the 12-valent cluster **5c** changes from 97 nM (at pH = 5.5) to 42 μM (at pH = 4), which corresponds to a factor of about 400. The higher valent cluster **5c** experiences indeed a much stronger change of the inhibition constant when lowering the pH, in line with our hypothesis. Or in tother words, the multivalent effect disappears at pH = 4 (ratio of inverse K_i is close to ratio of valency) most likely due to electrostatic effects.

Conclusions

In this work, we have developed an original approach to dissect key multivalent processes in glycosidase inhibition based on the top-down deconstruction of the current best-in-class multiheaded inhibitor. The unique combination of SAR studies, analytical experiments, and atomistic simulations provided relevant mechanistic insights. First, in this case study, tripling the local inhitope density – from cluster **4** to **1**, and from clusters **6a–c** to **5a–c**, respectively – increases the multivalent effect by one order of magnitude. Secondly, adequate structural requirements in terms of size and geometry do not necessarily lead to the formation of a cross-linked sandwich-type complex as shown by results obtained with 12-valent DNJ clusters **3** and **5a–c** and, to a lesser extent by the corresponding 4-valent clusters **6a–c**. DNJ head accessibility and the absence of topological restriction was indeed found to play a decisive role in generating 2:1 enzyme:inhibitor complexes, explaining why DNJ cluster **4** is the only 12-valent inhibitor of the series able to significantly cross–link two JBα-man molecules. While radial topology seems in principle valid for the studied neoglycoclusters, the corresponding thermodynamic model of Kitov and Bundle drastically underestimates the extent of the multivalent effect. The reason might be the partial protonation of the inhitopes. Results from pH-dependent simulations and inhibition experiments suggest that electrostatic interactions between the positively charged multivalent inhibitors and JBα-man have a significant impact on the multivalent effect. Considering the acidic pH inside lysosomes (pH < 5), these observations are of particular interest for the future design of

multiheaded iminosugar-based pharmacological chaperones targeting human lysosomal enzymes, including glycosidases.[40] Last but not least, the cumulative effects of chelating and clustering binding modes generated by the cross-linking of two JBα-man molecules is not a sufficient condition to reach outstanding levels of affinity enhancements as unambiguously demonstrated by the results obtained with DNJ cluster **4**. In the 12-valent inhibitor series, high local inhitope density (clusters **5**) or cross-linking ability (cluster **4**) lead to similar range inhibition values. It is the combination of both factors that leads to the supplementary gain of one order of magnitude (cluster **1**). Statistical rebinding effects should thus not be underestimated in the design of neoglycoclusters and the prevailing consensus on the leading role of the chelate effects over non–chelation binding modes must be subjected to more critical scrutiny. One way to optimize statistical rebinding could be to pursue high–valency clusters with inhitopes of equally high accessibility that are centrally anchored to the scaffold in a radial topology fashion. In this sense, unipod branches are a better choice than dendritic branches. High valency and radial topology should also favor the formation of the 2:1 complex since the degeneracy coefficient increases with the number of inhitopes and the number of active sites. Finally, the studied enzyme: inhibitor system of this deconstruction study is unique in the sense it offers two complementary dimensions (stoichiometry & electrostatics) to increase the multivalency effect in addition to the standard statistical dimension (i.e., degeneracy due to the multiple ways of forming microscopically distinguishable complexes). Optimizations along these additional dimensions is likely to improve the future design of multivalent inhibitors also for other receptor:ligand systems.

Experimental Section

All reactions were carried out in standard glassware or in vials adapted to a Biotage Initiator® microwave reactor and monitored by Thin Layer Chromatography on aluminium sheets coated with silica gel 60 F254 purchased from Merck KGaA. Visualization was accomplished with UV light (at 254 nm) and exposure to TLC stains. Crude mixtures were purified by flash chromatography on silica gel column (Silica gel 60, 230–400 mesh, 0.040–0.063 mm) purchased from E. Merck or by automated flash chromatography using a Grace Reveleris® flash system equipped with UV/Vis and ELSD detectors. HPLC analyses were performed on a JASCO LC-NET II/ADC equipped with a JASCO Model PU-2089 Plus Pump and a JASCO MD-2010 Plus UV-vis multiple wavelength detector set at 220 nm. The column used was a C18 reversed-phase analytical column (Waters, Bondapak, 10 μm, 125 Å, 3.9 mm×300 mm) run with linear gradients of ACN (0.1% TFA) into H_2O (0.1% TFA) over 30 min, at a flow rate of 1.0 mL/min for the analytical runs. Nuclear Magnetic Resonance (NMR) spectra were recorded on Bruker Avance 300 MHz, Bruker Avance III HD 400 MHz with BBFO probe or Bruker 500 MHz Avance III HD with Prodigy BBO probe spectrometers using solvent peaks as reference. Carbon multiplicities were assigned by Distortionless Enhancement by Polarization Transfer (DEPT) experiments. ^{1}H and ^{13}C signals were assigned by correlation spectroscopy (COSY), Heteronuclear Single Quantum Correlation (HSQC), and Heteronuclear Multiple-Bond Correlation spectroscopy (HMBC). Infrared (IR) spectra (cm^{-1}) were recorded neat on a Perkin-Elmer Spectrum One Spectrophotometer. ESI–TOF high resolution mass spectra (HRMS) were carried out on a Bruker MicroTOF spectrometer. MALDI mass spectra were carried out on a Bruker MALDI–TOF–TOF spectrometer. ESI–MS analysis in the positive-ion mode was performed using a Finnigan LCQ Deca ion trap mass spectrometer (ThermoFinnigan, San Jose', CA, USA), and the mass spectra were acquired and processed using the Xcalibur software provided by Thermo Finnigan. Specific rotations were determined on Anton Paar MCP 200 polarimeter with sodium lamp ($\lambda = 589$ nm) at 20 °C.

General procedure for the CuAAC reaction. To a 5 mL microwave vial containing the alkyne and azide (1.1 equiv/alkyne moiety) in DMF (1 to 3 mL) was added a bright yellow suspension of $CuSO_4 \cdot 5H_2O$ (0.1 equiv/alkyne moiety) and sodium ascorbate (0.2 equiv/alkyne moiety) in water (0.2 to 1 mL). The mixture was stirred and heated under microwave irradiation at 80 °C for 50 min to 1.5 h. The mixture was concentrated under reduced pressure, diluted in a mixture of MeCN/H_2O/30 wt%-NH_4OH (9:1:1) and filtered with the same eluent (25 mL) on a small pad of SiO_2 (typically 1 to 3 cm thick). Blue copper salts remained on the top of the silica gel pad. The filtrate was evaporated under reduced pressure and then purified by flash chromatography (SiO_2, CH_2Cl_2/MeOH, 100:0 to 90:10) to afford clicked product.

General procedure for the deacetylation reaction. To a solution of acetylated iminosugar click cluster **28**–**32** in a 1:1 mixture of H_2O/MeOH (1 mL/μmol) was added Amberlite IRA400 (OH^-) (2.5*n* to 6*n* g/mmol of substrate; n = number of acetate groups). The suspension was gently stirred overnight between 25 to 40 °C. The mixture was filtered, the resin washed with MeOH then water and the filtrate was concentrated under reduced pressure to afford deprotected iminosugar click cluster **3**–**7** as yellowish oil.

Synthesis of compound 8' (Figure S1). 2-Chlorotrityl chloride resin (2,α-dichlorobenzhydryl-polystyrene cross-linked with 1% DVB; 100–200 mesh; 1.63 mmol g^{-1}, 400 mg, 0.652 mmol) was washed with DCM (3×4 mL) and DMF (3×4 mL) and then swelled in dry DCM (4 mL) for 45 min. Bromoacetic acid (145 mg, 1.04 mmol) and DIPEA (0.600 mL, 3.26 mmol) in dry DCM (4 mL) were added to the resin and the vessel was stirred on a shaker platform for 60 min at room temperature. After the resin was washed with DMF (3×4 mL), DCM (3×4 mL) and then with DMF (3×4 mL), a solution of propargylamine (0.42 mL, 6.52 mmol) in dry DMF (4 mL) was added to the bromoacetylated resin. The mixture was left on the shaker platform for 40 min at room temperature, and then the resin was washed with DMF (3×4 mL), DCM (3×4 mL) and then with DMF (3×4 mL). Subsequent bromoacetylation reaction was accomplished by reacting the oligomer with a solution of bromoacetic acid (906 mg, 6.52 mmol) and DIC (1.11 mL, 7.17 mmol) in dry DMF (2 mL), stirring on a shaker platform for 40 min at room temperature. Then the reaction with the proper amine (methoxyethyl amine (0.57 mL, 6.52 mmol) or propargyl amine (0.42 mL, 6.52 mmol)) was realized as described above. The synthesis proceeded until the linear target was obtained. The oligomer-resin was cleaved by treatment with three aliquots of a solution of 20% HFIP in dry DCM (v/v; 3×4 mL), with stirring each time on the shaker platform for 30 min at room temperature and filtering the resin away after each treatment. The combined filtrates were concentrated in vacuo. The crude white amorphous solid (886 mg, >98%) was analyzed by ESI mass spectrometry and RP–HPLC and used for the cyclization step without further purification. RP–HPLC analysis Bondapak, 5% B in A→100% B in 30 min (A: 0.1% TFA in water, B: 0.1% TFA in acetonitrile), 1.0 mL/min, 220 nm, tr 12.9 min. MS (ESI) $[M+H]^+$ 1359.1.

Compound 8: To a stirred solution of HATU (1062 mg, 2.80 mmol) and DIPEA (760 μL, 4.34 mmol) in dry DMF (210 mL) at rt, was added a solution of the linear precursor **8'** (0.65 mmol) in dry DMF

(20 mL) using a syringe pump over 3 h. After 18 h, the resulting mixture was concentrated in vacuo, diluted with DCM (100 mL) and washed with 1 M HCl (2×50 mL). The aqueous layer was extracted with DCM (2×100 mL) and the combined organic phases were washed with water (150 mL), dried over $MgSO_4$ and concentrated in vacuo. The crude cyclic peptoid was purified by flash chromatography (SiO_2, petroleum ether:EtOAc 100:0 to 0:100 then EtOAc:MeOH 100:0 to 50:50) to give **8** as an amorphous solid. (227 mg, 0.17 mmol, 26%). m.p. 165–166 °C. RP–HPLC analysis: Bondapak, 5% B in A→100% B in 30 min (A: 0.1% TFA in water, B: 0.1% TFA in acetonitrile), 1.0 mL/min, 220 nm, tr 14.8 min. ^{1}H NMR (400 MHz, $CDCl_3$, mixture of rotamers) δ: 4.26–3.92 (m, 28 H, NCHHCO, NCHHCO, NCH_2CCH), 3.33–2.92 (m, 70 H, $NCH_2CH_2OCH_3$, $NCH_2CH_2OCH_3$, $NCH_2CH_2OCH_3$), 2.30–2.08 (m, 2 H, NCH_2CCH). ^{13}C NMR (100 MHz, $CDCl_3$, mixture of rotamers) δ: 169.9, 169.6, 169.4, 169.3, 169.2, 169.2, 169.0, 168.9, 168.8, 168.7, 168.7, 168.6, 168.6, 168.5, 168.4, 168.2, 168.2, 168.1, 168.0, 167.8, 167.7, 167.5, 167.3, 78.4, 78.3, 78.2, 78.2, 72.7, 72.6, 72.5, 72.4, 71.4, 70.8, 70.7, 70.0, 69.7, 69.6, 69.3, 58.6 (×2), 58.3 (×2), 58.1, 50.2, 50.0, 49.8, 49.7, 49.5, 47.8, 47.7, 47.6, 47.3, 37.8, 37.7, 37.5, 37.4, 37.3, 37.2, 37.1, 37.0, 37.0, 36.7, 36.6, 36.2, 36.0, 35.9, 35.8, 35.5. HRMS (MALDI) $[M+Na]^+$ calcd for $C_{60}H_{100}N_{12}NaO_{22}$, 1363.6967, found 1363.6989.

Compound 17: To a solution of **16**[22] (3 mmol) and n-Bu_4NHSO_4 (3 mmol) in 2-chloroethyl ether (9 mL) was added 50% aq. NaOH (9 mL). The biphasic reaction mixture was vigorously stirred at 35 °C for 22 h. The reaction mixture was diluted with Et_2O (80 mL), washed with water (2×30 mL) and brine (30 mL), then dried over Na_2SO_4, filtered and concentrated. Purification by flash column chromatography (Pentane/Et_2O 98:2 to 90:10 to elute excess residual 2-chloroethyl ether, then 90:10 to 80:20 to elute product) yielded **17** as a colorless oil (460 mg, 62%). R_f=0.31 (pentane/Et_2O 9:1). ^{1}H NMR (500 MHz, $CDCl_3$) δ 4.13 (d, J=2.4 Hz, 2 H), 3.77 (t, J=5.9 Hz, 2 H), 3.66 (dd, J=5.9, 3.7 Hz, 2 H), 3.63 (t, J=5.9 Hz, 2 H), 3.59 (dd, J=5.9, 3.7 Hz, 2 H), 3.28 (s, 2 H), 3.23 (s, 2 H), 2.39 (t, 1 H, J=2.4 Hz), 0.91 (s, 6 H). ^{13}C NMR (125 MHz, $CDCl_3$) δ 80.4, 77.4, 76.3, 74.0, 71.5, 71.2, 70.7, 58.7, 43.0, 36.3, 22.3 (2 C). HRMS (m/z) calcd for $[C_{12}H_{21}ClO_3+Na]^+$: 271.1071, found: 271.1058.

Compound 19: Compound **19** (199.3 mg, 0.27 mmol, 98%) was obtained as a pale-yellow oil according to the general procedure for CuAAC reaction, starting from clickable arm **17** (68 mg, 0.27 mmol) and the *N*-nonyl deoxynoririmycin azide derivative **18**[21] (150 mg, 0.3 mmol, 1.1 eq.). R_f=0.41 (DCM/MeOH 95:3). $[\alpha]_D^{20}$ = + 6.0 (c=1.2, $CHCl_3$). ^{1}H-NMR ($CDCl_3$, 500 MHz): δ 7.48 (s, 1H, H-16), 5.07–4.99 (m, 2H, H-3, H-4), 4.96–4.91 (m, 1H, H-2), 4.60 (s, 2H, H-18), 4.32 (t, J=7.3 Hz, 2H, H-15), 4.16–4.13 (m, 2H, H-6), 3.73 (t, J=5.8 Hz, 2H, H-24), 3.63–3.58 (m, 4H, H-23 and H-25), 3.56–3.54 (m, 2H, H-22), 3.26 (s, 2H, H-19), 3.20 (s, 2H, H-21), 3.17 (dd, J=11.0, 5.0 Hz, 1H, H-1a), 2.72–2.67 (m, 1H, H-7a), 2.61 (d, J=9.0 Hz, H-5), 2.55–2.51 (m, 1H, H-7b), 2.30 (t, J=10.8 Hz, 1H, H-1b), 2.05 (s, 3H, C(O)CH_3), 2.00 (s, 6H, C(O)CH_3), 1.98 (s, 3H, C(O)CH_3), 1.90–1.85 (m, 2H, H-14), 1.43–1.15 (m, 12H, H-8 to H-13), 0.87 (s, 6H, CH_3) ppm. ^{13}C-NMR ($CDCl_3$, 125 MHz): δ 170.99, 170.43, 170.11, 169.81, 145.86, 122.04, 77.37, 76.69, 74.77, 71.46, 71.15, 70.64, 69.60, 69.51, 65.24, 61.54, 59.59, 52.99, 51.84, 50.38, 43.02, 36.38, 30.40, 29.42, 29.01, 27.21, 26.57, 24.75, 22.25, 20.96, 20.92, 20.83, 20.77 ppm. IR (neat): 1746 cm^{-1}. MS (ESI) m/z calcd for $C_{35}H_{59}ClN_4O_{11}$ $[M+H]^+$ 747.3942; found 747.3940.

Compound 15: To a solution of halide **19** (137 mg, 0.18 mmol) in DMF (13 mL) was added NaN_3 (129 mg, 2 mmol, 10.8 eq.) and Bu_4NI (24 mg, 0.06 mmol, 0.35 eq.). The resulting mixture was heated to 80 °C for 20 h. Water (50 mL) was poured into the reaction mixture which was then extracted with EtOAc (3×50 mL). The organic layers were combined, washed with brine (50 mL), dried with $MgSO_4$ and evaporated. The crude was purified by flash chromatography (SiO_2; CH_2Cl_2/MeOH, 99:1 to 95:5) to give the desired product (131.3 mg, 0.17 mmol, 95%) as a pale-yellow oil. R_f=0.79 (DCM/MeOH 95:5). $[\alpha]_D^{20}$ = + 5.0 (c=1.8, $CHCl_3$). ^{1}H-NMR (500 MHz, $CDCl_3$): δ 7.47 (s, 1H, H-16), 5.07-4.99 (m, 2H, H-3, H-4), 4.96–4.91 (m, 1H, H-2), 4.59 (s, 2H, H-18), 4.31 (t, J=7.3 Hz, 2H, H-15), 4.13 (s, 2H, H-6), 3.65 (t, J=5.0 Hz, 2H, H-24), 3.62–3.60 (m, 2H, H-23), 3.56–3.54 (m, 2H, H-22), 3.34 (t, J=5.3 Hz, 2H, H-25), 3.26 (s, 2H, H-19), 3.21 (s, 2H, H-21), 3.17 (dd, J=11.0, 5.5 Hz, 1H, H-1a), 2.73–2.67 (m, 1H, H-7a), 2.61 (d, J=8.5 Hz, 1H, H-5), 2.55–2.50 (m, 1H, H-7b), 2.30 (t, J=10.8 Hz, 1H, H-1b), 2.04 (s, 3H, C(O)CH_3), 1.99 (s, 6H, C(O)CH_3), 1.98 (s, 3H, C(O)CH_3), 1.89–1.82 (m, 2H, H-14), 1.40–1.20 (m, 12H, H-8 to H-13), 0.86 (s, 6H, CH_3) ppm. ^{13}C-NMR ($CDCl_3$, 125 MHz): δ 171.03, 170.47, 170.14, 169.85, 145.91, 122.05, 77.41, 76.74, 74.80, 71.22, 70.72, 70.20, 69.62, 69.53, 65.27, 61.56, 59.61, 53.01, 51.86, 50.91, 50.40, 36.42, 30.43, 29.45, 29.04, 27.23, 26.59, 24.77, 22.25, 20.98, 20.95, 20.85, 20.79 ppm. IR (neat): 2107, 1744 (cm^{-1}). MS (ESI) m/z calcd for $C_{35}H_{60}N_7O_{11}$ $[M+H]^+$ 754.4345; found 754.4360.

Compound 21: Sodium hydride (60 w% in oil, 49 mg, 1.23 mmol) was added portionwise to a solution of alcohol **20**[23] (211 mg, 0.65 mmol) in THF (2.5 mL) at 0 °C. The mixture was stirred at rt for 2 h. A solution of 2-(2-chloroethoxy)ethyl triflate[24] (239 mg, 0.90 mmol) in THF (2.5 mL) was then added dropwise to the mixture at 0 °C. After 1.5 h of stirring at 0 °C, the reaction temperature was warmed to rt and stirred for 24 h. The reaction was quenched by adding MeOH (3 mL), and then the solution was concentrated in vacuo to give a residue, which was dissolved with DCM. The suspension was filtered through a small pad of SiO_2 and the filtrate was concentrated to give a residue which was purified by column chromatography (pentane/EtOAc, 5:1) to afford compound **21** (218 mg, 78%) as an oil. R_f=0.81 (Pentane/EtOAc 5:1). ^{1}H-NMR ($CDCl_3$, 500 MHz): δ 4.11 (d, J=2.5 Hz, 4H, H-3), 3.76 (t, J=5.75 Hz, 2H, H-10), 3.66–3.58 (m, 6H, H-7 to H-9), 3.57 (s, 2H, H-11), 3.49 (s, 4H, H-4), 3.43 (s, 2H, H-6), 2.39 (t, J=2.5 Hz, 2H, H-1), 0.88 (s, 9H, CCH_3), 0.03 (s, 6H, SiCH_3) ppm. ^{13}C-NMR ($CDCl_3$, 125 MHz): δ 80.32, 74.08, 71.50, 71.26, 70.63, 69.83, 69.07, 61.56, 58.84, 45.91, 42.98, 26.03, 18.39, −5.46 ppm. IR (neat): 3297,1092 (cm^{-1}). MS (ESI) m/z calcd for $C_{21}H_{37}ClNaO_5Si$ $[M+Na]^+$ 455.1991; found 455.1991.

Compound 22: To a solution of compound **21** (200 mg, 0.46 mmol) in dry THF (10 mL) at 0 °C was added dropwise a solution of TBAF in THF (1 M in THF, 1.85 mL, 1.85 mmol) over 15 min. The reaction mixture was allowed to warm to rt and stirred for 3.5 h under argon atmosphere. The solvent was evaporated under reduced pressure. The residue was diluted with EtOAc and washed with aqueous saturated NH_4Cl (2×50 mL) then with brine. The organic layers were dried over Na_2SO_4, and concentrated in vacuo to give a residue which was purified by column chromatography (pentane/EtOAc, 4:1) to afford compound **22** (143 mg, 0.45 mmol) as a pale-yellow sticky oil in 97% yield. R_f=0.13 (Pentane/EtOAc 4:1). ^{1}H-NMR ($CDCl_3$, 400 MHz): δ 4.13 (d, J=2.4 Hz, 4H, H-3), 3.75 (t, J=6.0 Hz, 2H, H-10), 3.70 (s, 2H, H-11), 3.67–3.60 (m, 6H, H-7 to H-9), 3.56 (s, 4H, H-4), 3.54 (s, 2H, H-6), 2.42 (t, J=2.4 Hz, H-1) ppm. ^{13}C-NMR ($CDCl_3$, 100 MHz): δ 79.89, 74.54, 71.90, 71.46, 71.09, 70.49, 70.31, 65.46, 58.94, 44.94, 42.92 ppm. IR (neat): 3484, 3293, 1090 (cm^{-1}). MS (ESI) m/z calcd for $C_{15}H_{23}ClNaO_5$ $[M+Na]^+$ 341.1126; found 341.1113.

Compound 23: To a solution of compound **22** (140 mg, 0.44 mmol) and (triisopropylsilyl)propargyl bromide (181 mg, 0.66 mmol) in dry THF (9 mL) was added sodium hydride (60 w% in oil, 26.4 mg, 0.66 mmol) at 0 °C, then the mixture was allowed to warm to rt and was stirred for 24 h. After quenching the reaction with MeOH (3 mL), the solvent was evaporated under reduced pressure. The residue was diluted with NH_4Cl and extracted with EtOAc (3×50 mL). The combined organic layers were washed with brine, dried over Na_2SO_4, and concentrated under reduced pressure. The crude residue was purified by column chromatography (pentane/EtOAc, 4:1) to afford **23** (152 mg, 0.30 mmol, 67%) as an oil. R_f=

0.87 (Pentane/EtOAc 4:1). ^{1}H-NMR ($CDCl_3$, 400 MHz): δ 4.15 (s, 2H, H-12), 4.11 (d, J=2.4 Hz, 4H, H-3), 3.76 (t, J=6.0 Hz, 2H, H-10), 3.66–3.57 (m, 6H, H-7 to H-9), 3.55 (s, 2H, H-11), 3.53 (s, 4H, H-4), 3.47 (s, 2H, H-6), 2.38 (t, J=2.4 Hz, 2H, H-1), 1.08–1.07 (m, 21H, $CH(CH_3)_2$) ppm. ^{13}C-NMR ($CDCl_3$, 100 MHz): δ 103.91, 87.34, 80.27, 74.10, 71.49, 71.27, 70.57, 70.26, 69.45, 69.01, 59.57, 58.85, 45.05, 42.99, 18.75, 11.33 ppm. IR (neat): 3302, 1095 (cm^{-1}). MS (ESI) m/z calcd for $C_{27}H_{45}ClNaO_5Si$ $[M+Na]^+$ 535.2617; found 535.2615.

Compound 24: Compound **24** (271 mg, 0.28 mmol, 97%) was obtained as a colorless oil according to the general procedure for CuAAC reaction, starting from compound **23** (150 mg, 0.29 mmol) and the tetraethyleneglycol azide[27] (141 mg, 0.64 mmol). R_f=0.5 (DCM/MeOH 9:1). ^{1}H-NMR ($CDCl_3$, 400 MHz): δ 7.72 (s, 2H, H-9), 4.58 (s, 4H, H-11), 4.53 (t, J=5.2 Hz, 4H, H-8), 4.12 (s, 2H, H-20), 3.87 (t, J=5.0 Hz, 4H, H-7), 3.74–3.70 (m, 6H, H-1 and H-18), 3.66–3.53 (m, 28H, H-15, H-16, from H-2 to H-6, H-17 and H-19), 3.49 (s, 4H, H-12), 3.44 (s, 2H, H-14), 1.05 (s, 21H, $CH(CH_3)_2$) ppm. ^{13}C-NMR ($CDCl_3$, 100 MHz): δ 145.41, 123.79, 103.93, 87.31, 72.66, 71.43, 71.16, 70.70, 70.64, 70.57, 70.52, 70.40, 70.22, 69.67, 69.63, 69.09, 65.19, 61.76, 59.56, 50.30, 45.35, 43.07, 18.72, 11.28 ppm. IR (neat): 3433, 1092 (cm^{-1}). MS (ESI) m/z calcd for $C_{43}H_{79}ClN_6NaO_{13}Si$ $[M+Na]^+$ 973.5055; found 973.5064.

Compound 25: To a solution of compound **24** (257 mg, 0.27 mmol) in anhydrous MeCN (2.9 mL) was added AgF (51.3 mg, 0.40 mmol) under argon in the dark. The mixture was stirred for 6 h in the dark at rt and then 1 M HCl (2.7 mL, 2.7 mmol) was added. The mixture was stirred for 5 min, diluted with water then extracted with DCM (5×50 mL). The combined organic layers were dried over Na_2SO_4, and concentrated under reduced pressure. The crude residue was purified by column chromatography (DCM/MeOH, 9:1) to give compound **25** (182 mg, 0.23 mmol, 85%) as a colorless oil. R_f=0.48 (DCM/MeOH 9:1). ^{1}H-NMR ($CDCl_3$, 400 MHz): δ 7.76 (s, 2H, H-9), 4.60 (s, 4H, H-11), 4.54 (t, J=5.2 Hz, 4H, H-8), 4.08 (d, J=2.4 Hz, 2H, H-20), 3.88 (t, J=5.0 Hz, 4H, H-7), 3.75–3.71 (m, 6H, H-1 and H-18), 3.66–3.54 (m, 28H, H-15, H-16, from H-2 to H-6, H-17 and H-19), 3.50 (br s, 4H, H-12), 3.44 (s, 2H, H-14), 2.44 (t, J=2.2 Hz, H-22) ppm. ^{13}C-NMR ($CDCl_3$, 100 MHz): δ 145.35, 123.94, 80.33, 74.43, 72.67, 71.45, 71.18, 70.71, 70.65, 70.57, 70.55, 70.41, 69.96, 69.68, 69.39, 69.20, 65.16, 61.78, 58.80, 50.37, 45.40, 43.11 ppm. IR (neat): 3435, 3259, 1092 (cm^{-1}). MS (ESI) m/z calcd for $C_{34}H_{59}ClN_6NaO_{13}$ $[M+Na]^+$ 817.3721; found 817.3700.

Compound 26: Compound **26** (197 mg, 0.15 mmol, 96%) was obtained as an oil according to the general procedure for CuAAC reaction, starting from compound **25** (126 mg, 0.16 mmol) and the *N*-nonyl deoxynoririmycin azide derivative **18**[21] (86.9 mg, 0.17 mmol, 1.1 eq.). R_f=0.72 (DCM/MeOH 9:1). ^{1}H-NMR ($CDCl_3$, 400 MHz): δ 7.74 (s, 2H, H-9′), 7.55 (s, 1H, H-16), 5.10-4.93 (m, 3H, H-2 to H-4), 4.56 (s, 6H, H-11′ and H-18), 4.53 (t, J=5.2 Hz, 4H, H-8′), 4.32 (t, J=7.4 Hz, 2H, H-15), 4.15 (s, 2H, H-6), 3.87 (t, J=5.2 Hz, 4H, H-7′), 3.73–3.70 (m, 6H, H-1′ and H-25), 3.65–3.51 (m, 28H, H-22, H-23, from H-2′ to H-6′, H-24 and H-19), 3.48–3.47 (m, 4H, H-12′), 3.43 (s, 2H, H-21), 3.19 (dd, J=11.6, 5.2 Hz, 1H, H-1a), 2.75–2.68 (m, 1H, H-7a), 2.63 (d, J=8.4 Hz, 1H, H-5), 2.58–2.52 (m, 1H, H-7b), 2.32 (t, J=10.6 Hz, 1H, H-1b), 2.07–2.00 (m, 12H, $COCH_3$), 1.91–1.87 (m, 2H, H-14), 1.42–1.26 (m, 12H, H-8 to H-13) ppm. ^{13}C-NMR ($CDCl_3$, 100 MHz): δ 171.05, 170.49, 170.16, 169.86, 145.51, 145.28, 123.93, 122.44, 74.81, 72.67, 71.42, 71.14, 70.70, 70.63, 70.56, 70.52, 70.40, 69.98, 69.64, 69.61, 69.55, 69.52, 69.46, 69.35, 65.30, 65.08, 61.74, 61.56, 59.61, 53.04, 51.92, 50.43, 50.28, 45.51, 43.14, 30.50, 29.52, 29.11, 27.29, 26.66, 24.76, 21.01, 20.98, 20.88, 20.82 ppm. IR (neat): 3471, 1745, 1096 (cm^{-1}). MS (ESI) m/z calcd for $C_{57}H_{98}ClN_{10}O_{21}$ $[M+H]^+$ 1293.6591; found 1293.6559.

Compound 27: To a solution of halide **26** (197 mg, 0.15 mmol) in DMF (8 mL) was added NaN_3 (107 mg, 1.6 mmol) and Bu_4NI (20 mg, 0.05 mmol). The resulting mixture was heated to 80 °C for 20 h. H_2O (10 mL) was poured into the reaction, which was then extracted with EtOAc (3×15 mL). The organic layers were combined, washed with brine (50 mL), dried with $MgSO_4$ and evaporated. The crude was purified by flash chromatography (SiO_2; CH_2Cl_2/MeOH, 99:1 to 95:5) to give the desired product (183 mg, 0.14 mmol, 92%) as a yellow oil. R_f=0.69 (DCM/MeOH 9:1). ^{1}H-NMR ($CDCl_3$, 500 MHz): δ 7.74 (s, 2H, H-9′), 7.55 (s, 1H, H-16), 5.09–4.93 (m, 3H, H-2 to H-4), 4.56 (s, 6H, H-11′ and H-18), 4.53 (t, J=5.3 Hz, 4H, H-8′), 4.32 (t, J=7.3 Hz, 2H, H-15), 4.14 (s, 2H, H-6), 3.87 (t, J=5.3 Hz, 4H, H-7′), 3.71 (t, J=4.5 Hz, 4H, H-1′), 3.65–3.48 (m, 32H, H-22, H-23, from H-2′ to H-6′, H-24, H-19 and H-12′), 3.44 (s, 2H, H-21), 3.34 (t, J=5.0 Hz, 2H, H-25), 3.18 (dd, J=11.5, 5.0 Hz, 1H, H-1a), 2.74–2.68 (m, 1H, H-7a), 2.63 (d, J=9.0 Hz, 1H, H-5), 2.57–2.52 (m, 1H, H-7b), 2.32 (t, J=10.8 Hz, 1H, H-1b), 2.06–2.00 (m, 12H, $COCH_3$), 1.90–1.88 (m, 2H, H-14), 1.43–1.26 (m, 12H, H-8 to H-13) ppm. ^{13}C-NMR ($CDCl_3$, 125 MHz): δ 171.05, 170.49, 170.16, 169.86, 145.52, 145.29, 123.92, 122.42, 74.82, 72.66, 71.15, 70.69, 70.62, 70.55, 70.40, 70.15, 70.01, 69.64, 69.56, 69.55, 69.52, 69.47, 69.35, 65.29, 65.07, 61.73, 61.55, 59.62, 53.05, 51.92, 50.90, 50.42, 50.27, 45.51, 30.49, 29.52, 29.11, 27.29, 26.65, 24.76, 21.00, 20.97, 20.88, 20.81 ppm. IR (neat): 3457, 2106, 1744, 1093 (cm^{-1}). MS (ESI) m/z calcd for $C_{57}H_{97}N_{13}NaO_{21}$ $[M+Na]^+$ 1322.6814; found 1322.6808.

Ligand 14: To a solution of compound **27** (100 mg, 0.077 mmol) in pyridine (1 mL) under argon, acetic anhydride (0.22 mL, 2.33 mmol) was added dropwise. The reaction mixture was stirred at rt for 26 h and then quenched with ice-cold water. The solution was stirred for 30 min, then poured into water, extracted with DCM (3×25 mL). The combined organic layers were washed with 1 M HCl (2×25 mL), then with $NaHCO_3$ (25 mL), dried over Na_2SO_4, and concentrated under reduced pressure. The crude residue was purified by column chromatography (DCM/MeOH, 9:1) to obtain compound **14** (104 mg, 0.075 mmol, 98%) as a pale-yellow oil. R_f=0.81 (DCM/MeOH 9:1). $[\alpha]_D^{20}$ = +1.5 (c=0.4, $CHCl_3$). ^{1}H-NMR ($CDCl_3$, 400 MHz): δ 7.69 (s, 2H, H-9′), 7.54 (s, 1H, H-16), 5.09–4.93 (m, 3H, H-2 to H-4), 4.55 (s, 6H, H-11′ and H-18), 4.52 (t, J=5.4 Hz, 4H, H-8′), 4.32 (t, J=7.4 Hz, 2H, H-15), 4.20 (t, J=4.8 Hz, 4H, H-1′), 4.15 (s, 2H, H-6), 3.87 (t, J=5.4 Hz, 4H, H-7′), 3.69–3.48 (m, 32H, H-22, H-23, from H-2′ to H-6′, H-24, H-19 and H-12′), 3.43 (s, 2H, H-21), 3.34 (t, J=5.0 Hz, 2H, H-25), 3.19 (dd, J=11.4, 5.0 Hz, 1H, H-1a), 2.75–2.68 (m, 1H, H-7a), 2.63 (d, J=8.0 Hz, 1H, H-5), 2.58–2.52 (m, 1H, H-7b), 2.32 (t, J=10.8 Hz, 1H, H-1b), 2.06–2.00 (m, 18H, $COCH_3$), 1.91–1.87 (m, 2H, H-14), 1.42–1.24 (m, 12H, H-8 to H-13) ppm. ^{13}C-NMR ($CDCl_3$, 100 MHz): δ 171.12, 171.04, 170.49, 170.15, 169.86, 145.54, 145.34, 123.69, 122.38, 74.82, 71.16, 70.68, 70.57, 70.16, 70.02, 69.63, 69.57, 69.55, 69.53, 69.48, 69.38, 69.27, 65.33, 65.10, 63.67, 61.57, 59.62, 53.04, 51.92, 50.90, 50.40, 45.52, 30.50, 29.53, 29.12, 27.30, 26.66, 24.78, 21.10, 21.01, 20.98, 20.88, 20.82 ppm. IR (neat): 2107, 1741 (cm^{-1}). MS (ESI) average m/z calcd for $C_{61}H_{101}N_{13}NaO_{23}$ $[M+Na]^+$ 1406.7025; found 1406.6991.

Acetylated cluster 28: Compound **28** (45 mg, 2.5 μmol, 53%) was prepared as a colorless oil according to the general procedure, starting from cyclopeptoid **12** (5.5 mg, 4.8 μmol) and ligand **14** (100 mg, 72.3 μmol). R_f=0.56 (DCM/MeOH 9:1). $[\alpha]_D^{20}$ = +1.0 (c=1.0, $CHCl_3$). ^{1}H-NMR ($CDCl_3$, 500 MHz): δ 8.40–7.75 (br s, 12H, H-26), 7.71 (s, 24H, H-9′), 7.59 (s, 12H, H-16), 5.07–4.99 (m, 24H, H-3 and H-4), 4.96-4.91 (m, 12H, H-2), 4.50–3.44 (m, 744H, H-6, H-15, H-18, H-19, H-21 to H-25, H-1′ to H-8′, H-11′, H-12′, H-28 and H-30), 3.17 (dd, J=11.3, 4.8 Hz, 12H, H-1a), 2.73–2.67 (m, 12H, H-7a), 2.62 (d, J=9.0 Hz, 12H, H-5), 2.57–2.51 (m, 12H, H-7b), 2.31 (t, J=10.8 Hz, 12H, H-1b), 2.05–1.99 (m, 216H, $COCH_3$), 1.87 (br s, 24H, H-14), 1.40–1.21 (m, 144H, H-8 to H-13) ppm. ^{13}C-NMR ($CDCl_3$, 125 MHz): δ 171.05, 170.99, 170.44, 170.11, 169.84, 145.31, 145.14, 142.80, 124.54, 123.80, 122.63, 74.81, 71.13, 70.95, 70.59, 70.23, 69.92, 69.62, 69.53, 69.37, 69.24, 69.18, 65.19, 64.98, 63.64, 61.50, 59.59, 53.04, 51.92,

50.35, 50.18, 45.46, 42.55, 30.51, 29.57, 29.14, 27.32, 26.68, 24.74, 21.06, 20.97, 20.94, 20.85, 20.78 ppm. IR (neat): 1741 (cm^{-1}). MS (ESI) average m/z calcd for $C_{792}H_{1282}N_{168}O_{288}$ $[M+10H]^{10+}$ 1776.5164; found 1776.5293.

Cluster 3: Compound **3** was obtained as a colorless oil in quantitative yield (31 mg, 2.1 μmol) from its acetylated precursor **28** (37 mg, 2.1 μmol) according to the general procedure. $[\alpha]_D^{20} = -3.0$ ($c = 1.6$, CH_3OH). ^{1}H-NMR (MeOD, 500 MHz): δ 8.23–8.00 (br s, 12H, H-26), 7.99 (s, 24H, H-9′), 7.59 (s, 12H, H-16), 4.55–3.30 (m, 840H, H-2, H-4, H-6, H-15, H-18, H-19, H-21 to H-25, H-1′ to H-8′, H-11′, H-12′, H-28, H-30), 3.14 (t, $J = 9.0$ Hz, 12H, H-3), 2.97 (dd, $J = 11.0$, 5.0 Hz, 12H, H-1a), 2.80–2.74 (m, 12H, H-7a), 2.57–2.52 (m, 12H, H-7b), 2.16 (t, $J = 11.0$ Hz, 12H, H-1b), 2.10 (d, $J = 9.5$ Hz, 12H, H-5), 1.87 (s, 24H, H-14), 1.48–1.45 (m, 24H, H-8), 1.34–1.27 (m, 120H, H-9 to H-13) ppm. ^{13}C-NMR (MeOD, 125 MHz): δ 170.27, 146.16, 146.01, 144.41, 143.64, 125.88, 125.77, 124.95, 80.63, 73.70, 72.20, 72.12, 71.55, 71.47, 71.40, 71.23, 70.81, 70.50, 70.41, 70.14, 67.39, 65.54, 65.49, 62.21, 59.60, 57.80, 53.78, 51.45, 51.36, 46.58, 43.70, 31.36, 30.54, 30.05, 28.60, 27.52, 25.26 ppm. IR (neat): 3381, 1669 (cm^{-1}). MS (ESI) average m/z calcd for $C_{648}H_{1138}N_{168}O_{216}$ $[M+10H]^{10+}$ 1473.8649; found 1473.8874.

Acetylated cluster 29: Acetylated compound **29** (30.3 mg, 3.0 μmol, 68%) was prepared as a pale-yellow oil according to the general procedure, starting from cyclopeptoid **12** (5 mg, 4.4 μmol) and ligand **15** (59 mg, 78.3 μmol). $R_f = 0.29$ (DCM/MeOH 100:8). $[\alpha]_D^{20} = +0.35$ ($c = 0.4$, $CHCl_3$). ^{1}H-NMR ($CDCl_3$, 500 MHz): δ 8.11–7.57 (m, 12H, H-26), 7.51 (s, 12H, H-16), 5.08–4.93 (m, 36H, H-3, H-4, and H-2), 4.70–2.98 (m, 276H, H-18, H-28, H-25, H-15, H-30, H-6, H-24, H-19, H-21 to H-23, H-1a), 2.74–2.68 (m, 12H, H-7a), 2.64 (d, $J = 8.8$ Hz, 12H, H-5), 2.58–2.49 (m, 12H, H-7b), 2.32 (t, $J = 10.8$ Hz, 12H, H-1b), 2.06 (s, 36H, C(O)CH_3), 2.01 (s, 72H, C(O)CH_3), 1.99 (s, 36H, C(O)CH_3), 1.92–1.83 (br s, 24H, H-14), 1.46–1.16 (m, 144H, H-8 to H-13), 0.84 (s, 72H, CH_3) ppm. ^{13}C-NMR ($CDCl_3$, 125 MHz): δ 171.02, 170.47, 170.14, 169.85, 145.72, 142.41, 124.50, 122.26, 74.79, 71.14, 70.48, 69.60, 69.50, 65.19, 61.56, 59.60, 53.00, 51.90, 50.42, 48.41, 42.49, 36.44, 30.47, 29.50, 29.09, 27.27, 26.63, 24.76, 22.28, 21.00, 20.97, 20.87, 20.81 ppm. IR (neat): 1746 (cm^{-1}). MS (ESI) average m/z calcd for $C_{480}H_{774}N_{96}O_{144}$ $[M+6H]^{6+}$ 1697.9360; found 1697.9332.

Cluster 4: Compound **4** was obtained as a pale-yellow oil in quantitative yield (24 mg, 3.0 μmol) from its acetylated precursor **29** (30.3 mg, 3.0 μmol) according to the general procedure. $[\alpha]_D^{20} = -6.0$ ($c = 1.0$, CH_3OH). ^{1}H-NMR (MeOD, 500 MHz): δ 8.15–7.90 (br s, 24H, H-26 and H-16), 4.65–3.07 (m, 348H, H-2 to H-4, H-6, H-15, H-18, H-19, H-21 to H-25, H-28, H-30 and OH), 2.97 (dd, $J = 11.1$, 4.8 Hz, 12H, H-1a), 2.80–2.74 (m, 12H, H-7a), 2.58–2.52 (m, 12H, H-7b), 2.16 (t, $J = 10.9$ Hz, 12H, H-1b), 2.10 (d, $J = 9.5$ Hz, 12H, H-5), 1.92–1.85 (br s, 24H, H-14), 1.48–1.44 (m, 24H, H-8), 1.36–1.22 (br s, 120H, H-9 to H-13), 0.83 (s, 72H, CH_3) ppm. ^{13}C-NMR (MeOD, 125 MHz): δ 170.30, 146.26, 144.10, 125.91, 124.91, 80.61, 78.22, 77.40, 72.11, 71.41, 70.81, 70.48, 67.38, 65.37, 59.57, 57.79, 53.79, 51.53, 51.35, 43.36, 37.25, 31.34, 30.54, 30.04, 28.61, 27.48, 25.25, 22.75 ppm. IR (neat): 3367, 1671 (cm^{-1}). MS (MALDI) 8171.18 ($C_{384}H_{673}N_{96}O_{96}$) $[M+H]^+$, found 8171.51; 8193.17 ($C_{384}H_{672}N_{96}NaO_{96}$) $[M+Na]^+$, found: 8194.71.

Acetylated cluster 30a: Acetylated compound **30a** (56 mg, 6.4 μmol, 79%) was prepared as a colorless oil according to the general procedure, starting from cyclopeptoid **9** (10.5 mg, 8.1 μmol) and ligand **13** (69 mg, 37.1 μmol). $R_f = 0.40$ (DCM/MeOH 95:5). $[\alpha]_D^{20} = +4.0$ ($c = 2.1$, $CHCl_3$). ^{1}H-NMR ($CDCl_3$, 500 MHz): δ 8.12–7.64 (br s, 4H, H-26), 7.53 (s, 12H, H-16), 5.06–4.98 (m, 24H, H-3 and H-4), 4.95–4.91 (m, 12H, H-2), 4.65–3.72 (m, 120H, H-18, H-28, H-25, H-15, H-30, H-6 and H-24), 3.63–3.10 (m, 116H, H-19, H-21 to H-23, H-31 to H-32, H-1a and OCH_3), 2.72–2.66 (m, 12H, H-7a), 2.61 (d, $J = 8.0$ Hz, 12H, H-5), 2.52 (br s, 12H, H-7b), 2.30 (t, $J = 10.8$ Hz, 12H, H-1b), 2.04 (s, 36H, C(O)CH_3), 1.99 (s, 72H, C(O)CH_3), 1.97 (s, 36H, C(O)CH_3), 1.86 (br s, 24H, H-14), 1.45–1.17 (m, 144H, H-8 to H-13) ppm. ^{13}C-NMR ($CDCl_3$, 125 MHz): δ 170.94, 170.39, 170.06, 169.78, 168.96, 145.29, 143.41, 124.31, 122.47, 74.73, 71.04, 70.33, 69.86, 69.54, 69.44, 69.29, 65.10, 61.48, 59.54, 59.09, 58.77, 52.95, 51.83, 50.34, 48.03, 45.39, 42.51, 30.42, 29.45, 29.04, 27.21, 26.58, 24.71, 20.92, 20.90, 20.80, 20.74 ppm. IR (neat): 1746, 1672 (cm^{-1}). MS (ESI) average m/z calcd for $C_{408}H_{657}N_{72}O_{136}$ $[M+9H]^{9+}$ 971.2962; found 971.2932.

Cluster 5a: Compound **5a** was obtained as a colorless oil in quantitative yield (38.5 mg, 5.7 μmol) from its acetylated precursor **30a** (50 mg, 5.7 μmol) according to the general procedure. $[\alpha]_D^{20} = -7.5$ ($c = 1.8$, CH_3OH). ^{1}H-NMR (MeOD, 500 MHz): δ 8.18–7.95 (br s, 4H, H-26), 7.94 (s, 12H, H-16), 4.79–3.88 (m, 88H, H-18, H-15, H-25, H-28 and H-30), 3.87–3.79 (m, 32H, H-6 and H-24), 3.56–3.27 (m, 128H, H-2, H-4, H-19, H-21 to H-23, H-31 to H-32 and OCH_3), 3.13 (t, $J = 9.0$ Hz, 12H, H-3), 2.98 (dd, $J = 11.0$, 4.5 Hz, 12H, H-1a), 2.80–2.75 (m, 12H, H-7a), 2.58–2.53 (m, 12H, H-7b), 2.16 (t, $J = 10.8$ Hz, 12H, H-1b), 2.10 (d, $J = 9.5$ Hz, 12H, H-5), 1.89 (s, 24H, H-14), 1.48-1.46 (m, 24H, H-8), 1.31 (s, 120H, H-9 to H-13) ppm. ^{13}C-NMR (MeOD, 125 MHz): δ 171.63, 146.14, 144.54, 125.82, 124.93, 80.61, 72.09, 71.32, 70.79, 70.45, 70.04, 67.38, 65.43, 59.57, 59.17, 57.78, 53.79, 51.51, 51.34, 49.86, 46.51, 43.48, 31.35, 30.54, 30.05, 28.60, 27.50, 25.24 ppm. IR (neat): 3380, 1668 (cm^{-1}). MS (ESI) average m/z calcd for $C_{312}H_{559}N_{72}O_{88}$ $[M+7H]^{7+}$ 960.4492; found 960.4471.

Acetylated cluster 30b: Acetylated compound **30b** (60 mg, 6.9 μmol, 63%) was prepared as a colorless oil according to the general procedure, starting from cyclopeptoid **10** (14.2 mg, 10.9 μmol) and ligand **13** (89.3 mg, 48 μmol). $R_f = 0.55$ (DCM/MeOH 9:1). $[\alpha]_D^{20} = +4.0$ ($c = 2.2$, $CHCl_3$). ^{1}H-NMR ($CDCl_3$, 500 MHz): δ 7.97–7.62 (br s, 4H, H-26), 7.53 (s, 12H, H-16), 5.06–4.98 (m, 24H, H-3 and H-4), 4.95–4.91 (m, 12H, H-2), 4.82–3.69 (m, 120H, H-18, H-28, H-25, H-15, H-30, H-6 and H-24), 3.66–2.87 (m, 116H, H-19, H-21 to H-23, H-31 to H-32, H-1a and OCH_3), 2.71–2.66 (m, 12H, H-7a), 2.60 (d, $J = 9.0$ Hz, 12H, H-5), 2.54–2.50 (m, 12H, H-7b), 2.29 (t, $J = 10.8$ Hz, 12H, H-1b), 2.04 (s, 36H, C(O)CH_3), 1.99 (s, 72H, C(O)CH_3), 1.98 (s, 36H, C(O)CH_3), 1.86 (s, 24H, H-14), 1.45–1.14 (m, 144H, H-8 to H-13) ppm. ^{13}C-NMR ($CDCl_3$, 125 MHz): δ 170.96, 170.41, 170.09, 169.80, 168.86, 145.31, 143.41, 124.13, 122.46, 74.78, 71.10, 70.32, 69.90, 69.60, 69.51, 69.31, 65.14, 61.51, 59.58, 59.08, 58.75, 53.00, 51.85, 50.36, 48.09, 45.42, 42.54, 30.44, 29.48, 29.07, 27.25, 26.61, 24.74, 20.95, 20.92, 20.82, 20.76 ppm. IR (neat): 1745, 1673 (cm^{-1}). MS (ESI) average m/z calcd for $C_{408}H_{654}N_{72}O_{136}$ $[M+6H]^{6+}$ 1456.4407; found 1456.4427.

Cluster 5b: Compound **5b** was obtained as a colorless oil in quantitative yield (32 mg, 4.8 μmol) from its acetylated precursor **30b** (42 mg, 4.8 μmol) according to the general procedure. $[\alpha]_D^{20} = -5.0$ ($c = 1.5$, CH_3OH). ^{1}H-NMR (MeOD, 500 MHz): δ 8.18–7.92 (br s, 4H, H-26), 7.90 (s, 12H, H-16), 4.63–3.65 (m, 120H, H-18, H-15, H-25, H-28, H-30, H-6 and H-24), 3.59–3.17 (m, 128H, H-2, H-4, H-19, H-21 to H-23, H-31, H-32 and OCH_3), 3.12–3.08 (m, 12H, H-3), 2.95–2.92 (m, 12H, H-1a), 2.76–2.71 (m, 12H, H-7a), 2.54–2.49 (m, 12H, H-7b), 2.12 (t, $J = 10.8$ Hz, 12H, H-1b), 2.06 (d, $J = 9.0$ Hz, 12H, H-5), 1.85 (s, 24H, H-14), 1.43 (m, 24H, H-8), 1.27 (s, 120H, H-9 to H-13) ppm. ^{13}C-NMR (MeOD, 125 MHz): δ 171.45, 146.13, 144.61, 125.65, 124.92, 80.60, 72.08, 71.33, 70.78, 70.45, 70.02, 67.37, 65.43, 59.56, 59.15, 57.77, 53.78, 51.50, 51.34, 49.86, 46.50, 43.66, 31.35, 30.54, 30.05, 28.60, 27.50, 25.23 ppm. IR (neat): 3366, 1668 (cm^{-1}). MS (ESI) average m/z calcd for $C_{312}H_{559}N_{72}O_{88}$ $[M+7H]^{7+}$ 960.4492; found 960.4510.

Acetylated cluster 30c: Acetylated compound **30c** (39 mg, 4.5 μmol, 55%) was prepared as a colorless oil according to the general procedure, starting from cyclopeptoid **11** (10.5 mg, 8.1 μmol) and ligand **13** (66 mg, 36 μmol). $R_f = 0.35$ (DCM/MeOH

92:8). $[\alpha]_D^{20} = +3.5$ ($c = 1.4$, $CHCl_3$). ^{1}H-NMR ($CDCl_3$, 500 MHz): δ 8.02–7.63 (br s, 4H, H-26), 7.54 (s, 12H, H-16), 5.07–5.00 (m, 24H, H-3 and H-4), 4.97–4.92 (m, 12H, H-2), 4.74–3.65 (m, 120H, H-18, H-28, H-25, H-15, H-30, H-6 and H-24), 3.63–3.10 (m, 116H, H-19, H-21 to H-23, H-31 to H-32, H-1a and OCH_3), 2.73–2.67 (m, 12H, H-7a), 2.62 (d, $J = 9.0$ Hz, 12H, H-5), 2.56–2.51 (m, 12H, H-7b), 2.30 (t, $J = 10.8$ Hz, 12H, H-1b), 2.05 (s, 36H, C(O)CH_3), 2.00 (s, 72H, C(O)CH_3), 1.99 (s, 36H, C(O)CH_3), 1.88 (br s, 24H, H-14), 1.42–1.15 (m, 144H, H-8 to H-13) ppm. ^{13}C-NMR ($CDCl_3$, 125 MHz): δ 171.02, 170.46, 170.13, 169.85, 168.96, 145.34, 143.53, 124.11, 122.49, 74.81, 71.14, 70.38, 69.94, 69.63, 69.54, 69.35, 65.17, 61.54, 59.61, 59.14, 58.81, 53.04, 51.89, 50.40, 48.13, 45.45, 42.50, 30.48, 29.52, 29.10, 27.28, 26.65, 24.78, 20.98, 20.96, 20.86, 20.80 ppm. IR (neat): 1745, 1673 (cm^{-1}). MS (ESI) average m/z calcd for $C_{408}H_{654}N_{72}O_{136}$ $[M+6H]^{6+}$ 1456.4407; found 1456.4396.

Cluster 5c: Compound **5c** was obtained as a colorless oil in 90% (18 mg, 2.7 μmol) from its acetylated precursor **30c** (26 mg, 3 μmol) according to the general procedure. $[\alpha]_D^{20} = -7.5$ ($c = 0.9$, CH_3OH). ^{1}H-NMR (MeOD, 500 MHz): δ 8.16–7.95 (br s, 4H, H-26), 7.94 (s, 12H, H-16), 4.69–3.93 (m, 88H, H-18, H-15, H-25, H-28 and H-30), 3.89–3.78 (m, 32H, H-6 and H-24), 3.60–3.21 (m, 128H, H-2, H-4, H-19, H-21 to H-23, H-31, H-32 and OCH_3), 3.13 (t, $J = 9.0$ Hz, 12H, H-3), 2.98 (dd, $J = 11.0$, 4.5 Hz, 12H, H-1a), 2.80–2.75 (m, 12H, H-7a), 2.58–2.53 (m, 12H, H-7b), 2.16 (t, $J = 11.0$ Hz, 12H, H-1b), 2.10 (d, $J = 9.5$ Hz, 12H, H-5), 1.89 (m, 24H, H-14), 1.48–1.46 (m, 24H, H-8), 1.31 (s, 120H, H-9 to H-13) ppm. ^{13}C-NMR (MeOD, 125 MHz): δ 171.49, 146.15, 144.55, 125.69, 124.93, 80.62, 72.09, 71.33, 70.80, 70.46, 70.03, 67.39, 65.42, 59.57, 59.16, 57.78, 53.79, 51.53, 51.35, 49.62, 46.48, 43.76, 31.36, 30.55, 30.05, 28.60, 27.50, 25.24 ppm. IR (neat): 3370, 1670 (cm^{-1}). MS (ESI) average m/z calcd for $C_{312}H_{560}N_{72}O_{88}$ $[M+8H]^{8+}$ 840.5189; found 840.5206.

Acetylated cluster 31a: Acetylated compound **31a** (68 mg, 16 μmol, 82%) was prepared as a colorless oil according to the general procedure, starting from cyclopeptoid **9** (25 mg, 19 μmol) and ligand **15** (63.7 mg, 85 μmol). $R_f = 0.54$ (DCM/MeOH 90:8). $[\alpha]_D^{20} = +3.0$ ($c = 2.1$, $CHCl_3$). ^{1}H-NMR ($CDCl_3$, 400 MHz): δ 8.02–7.56 (br s, 4H, H-26), 7.48 (s, 4H, H-16), 5.07–4.98 (m, 8H, H-3 and H-4), 4.96–4.90 (m, 4H, H-2), 4.78–3.64 (m, 72H, H-18, H-28, H-25, H-15, H-30, H-6 and H-24), 3.62–3.00 (m, 92H, H-19, H-21 to H-23, H-31 to H-32, H-1a and OCH_3), 2.73–2.66 (m, 4H, H-7a), 2.61 (d, $J = 8.4$ Hz, 4H, H-5), 2.56–2.49 (m, 4H, H-7b), 2.29 (t, $J = 10.6$ Hz, 4H, H-1b), 2.04 (s, 12H, C(O)CH_3), 1.99 (s, 24H, C(O)CH_3), 1.98 (s, 12H, C(O)CH_3), 1.87 (br s, 8H, H-14), 1.44-1.16 (m, 48H, H-8 to H-13), 0.84 (s, 24H, CH_3) ppm. ^{13}C-NMR ($CDCl_3$, 100 MHz): δ 170.98, 170.42, 170.10, 169.81, 168.92, 145.73, 142.30, 124.20, 122.12, 77.38, 76.72, 74.79, 71.08, 70.55, 69.62, 69.52, 65.19, 61.54, 59.61, 59.09, 58.83, 53.01, 51.84, 50.38, 48.31, 48.01, 42.51, 36.39, 30.42, 29.45, 29.04, 27.23, 26.59, 24.77, 22.23, 20.96, 20.93, 20.84, 20.78 ppm. IR (neat): 1746, 1673 (cm^{-1}). MS (ESI) average m/z calcd for $C_{200}H_{334}N_{40}O_{64}$ $[M+6H]^{6+}$ 720.0680; found 720.0701.

Cluster 6a: Compound **6a** was obtained as a colorless oil in quantitative yield (46 mg, 13 μmol) from its acetylated precursor **31a** (58 mg, 13 μmol) according to the general procedure. $[\alpha]_D^{20} = -4.5$ ($c = 2.2$, CH_3OH). ^{1}H-NMR (MeOD, 500 MHz): δ 8.17–7.96 (br s, 4H, H-26), 7.95 (s, 4H, H-16), 4.78–3.93 (m, 56H, H-18, H-15, H-25, H-28 and H-30), 3.90-3.76 (m, 16H, H-6 and H-24), 3.65–3.16 (m, 96H, H-2, H-4, H-19, H-21 to H-23, H-31, H-32 and OCH_3), 3.13 (t, $J = 9.0$ Hz, 4H, H-3), 2.98 (dd, $J = 11.0$, 4.5 Hz, 4H, H-1a), 2.81–2.75 (m, 4H, H-7a), 2.58–2.53 (m, 4H, H-7b), 2.16 (t, $J = 10.8$ Hz, 4H, H-1b), 2.10 (d, $J = 9.5$ Hz, 4H, H-5), 1.93–1.85 (br m, 8H, H-14), 1.49–1.46 (m, 8H, H-8), 1.31 (br s, 40H, H-9 to H-13), 0.85 (s, 24H, CH_3) ppm. ^{13}C-NMR (MeOD, 125 MHz): δ 171.61, 146.24, 144.26, 125.86, 124.87, 80.60, 78.17, 77.33, 72.07, 72.02, 71.41, 70.77, 70.42, 67.37, 65.27, 59.54, 59.43, 59.11, 57.74, 53.76, 51.49, 51.30, 43.56, 37.19, 31.29, 30.49, 29.98, 28.56, 27.43, 25.21, 22.64 ppm. IR (neat): 3400, 1667 (cm^{-1}). MS (ESI) average m/z calcd for $C_{168}H_{296}N_{40}Na_2O_{48}$ $[M+2Na]^{2+}$ 1844.0868; found 1844.0865.

Acetylated cluster 31b: Acetylated compound **31b** (54 mg, 13 μmol, 68%) was prepared as a colorless oil according to the general procedure, starting from cyclopeptoid **10** (24 mg, 18 μmol) and ligand **15** (63.7 mg, 85 μmol). $R_f = 0.43$ (DCM/MeOH 9:1). $[\alpha]_D^{20} = +4.0$ ($c = 0.7$, $CHCl_3$). ^{1}H-NMR ($CDCl_3$, 500 MHz): δ 8.06–7.59 (br s, 4H, H-26), 7.48 (s, 4H, H-16), 5.07–4.99 (m, 8H, H-3 and H-4), 4.96–4.91 (m, 4H, H-2), 4.85–3.57 (m, 72H, H-18, H-28, H-25, H-15, H-30, H-6 and H-24), 3.54–2.96 (m, 92H, H-19, H-21 to H-23, H-31 to H-32, H-1a and OCH_3), 2.73–2.67 (m, 4H, H-7a), 2.61 (d, $J = 9.0$ Hz, 4H, H-5), 2.54–2.51 (m, 4H, H-7b), 2.30 (t, $J = 11.0$ Hz, 4H, H-1b), 2.05 (s, 12H, C(O)CH_3), 2.00 (s, 24H, C(O)CH_3), 1.98 (s, 12H, C(O)CH_3), 1.88 (br s, 8H, H-14), 1.43-1.17 (m, 48H, H-8 to H-13), 0.84 (s, 24H, CH_3) ppm. ^{13}C-NMR ($CDCl_3$, 100 MHz): δ 170.99, 170.43, 170.11, 169.82, 169.00, 145.71, 143.21, 124.08, 122.13, 77.37, 76.71, 74.79, 71.08, 70.53, 69.61, 69.52, 65.18, 61.53, 59.60, 59.11, 58.84, 53.01, 51.85, 50.39, 48.48, 48.02, 42.44, 36.39, 30.43, 29.46, 29.05, 27.23, 26.59, 24.76, 22.24, 20.97, 20.94, 20.85, 20.78 ppm. IR (neat): 1746, 1673 cm^{-1}. MS (ESI) average m/z calcd for $C_{200}H_{331}N_{40}O_{64}$ $[M+3H]^{3+}$ 1439.1287; found 1439.1327.

Cluster 6b: Compound **6b** was obtained as a colorless oil in 92% yield (35 mg, 9.6 μmol) from its acetylated precursor **31b** (45 mg, 10.4 μmol) according to the general procedure. $[\alpha]_D^{20} = -4.0$ ($c = 1.7$, CH_3OH). ^{1}H-NMR (MeOD, 400 MHz): δ 8.20–7.96 (br s, 4H, H-26), 7.95 (s, 4H, H-16), 4.80–3.93 (m, 56H, H-18, H-15, H-25, H-28 and H-30), 3.89–3.76 (m, 16H, H-6 and H-24), 3.67–3.16 (m, 96H, H-2, H-4, H-19, H-21 to H-23, H-31, H-32 and OCH_3), 3.13 (t, $J = 9.2$ Hz, 4H, H-3), 2.98 (dd, $J = 11.2$, 4.8 Hz, 4H, H-1a), 2.82–2.74 (m, 4H, H-7a), 2.59–2.52 (m, 4H, H-7b), 2.16 (t, $J = 10.8$ Hz, 4H, H-1b), 2.10 (dt, $J = 9.6$, 2.4 Hz, 4H, H-5), 1.93–1.85 (m, 8H, H-14), 1.51–1.44 (m, 8H, H-8), 1.31 (s, 40H, H-9 to H-13), 0.85 (s, 24H, CH_3) ppm. ^{13}C-NMR (MeOD, 100 MHz): δ 171.13, 146.22, 144.21, 125.73, 124.86, 80.59, 78.17, 77.33, 72.07, 72.03, 71.40, 70.77, 70.44, 67.37, 65.27, 59.54, 59.43, 59.09, 57.75, 53.76, 51.50, 51.31, 43.60, 37.19, 31.30, 30.50, 29.99, 28.57, 27.44, 25.21, 22.65 ppm. IR (neat): 3414, 1669 (cm^{-1}). MS (ESI) average m/z calcd for $C_{168}H_{301}N_{40}O_{48}$ $[M+5H]^{5+}$ 729.4463; found 729.4475.

Acetylated cluster 31c: Acetylated compound **31c** (60 mg, 14 μmol, 72%) was prepared as a colorless oil according to the general procedure, starting from cyclopeptoid **11** (25 mg, 19 μmol) and ligand **15** (63.7 mg, 85 μmol). $R_f = 0.58$ (DCM/MeOH 9:1). $[\alpha]_D^{20} = +3.0$ ($c = 2.4$, $CHCl_3$). ^{1}H-NMR ($CDCl_3$, 400 MHz): δ 8.06–7.55 (br s, 4H, H-26), 7.48 (s, 4H, H-16), 5.06–4.98 (m, 8H, H-3 and H-4), 4.95–4.90 (m, 4H, H-2), 4.69–3.63 (m, 72H, H-18, H-28, H-25, H-15, H-30, H-6 and H-24), 3.61–3.05 (m, 92H, H-19, H-21 to H-23, H-31 to H-32, H-1a and OCH_3), 2.72–2.65 (m, 4H, H-7a), 2.60 (d, $J = 8.4$ Hz, 4H, H-5), 2.55–2.48 (m, 4H, H-7b), 2.29 (t, $J = 10.8$ Hz, 4H, H-1b), 2.04 (s, 12H, C(O)CH_3), 1.99 (s, 24H, C(O)CH_3), 1.98 (s, 12H, C(O)CH_3), 1.87 (br s, 8H, H-14), 1.42–1.15 (m, 48H, H-8 to H-13), 0.83 (s, 24H, CH_3) ppm. ^{13}C-NMR ($CDCl_3$, 100 MHz): δ 170.97, 170.41, 170.09, 169.80, 168.86, 145.70, 143.25, 124.14, 122.11, 77.36, 76.69, 74.77, 71.06, 70.54, 69.60, 69.51, 65.16, 61.53, 59.59, 59.07, 58.82, 52.99, 51.83, 50.36, 48.36, 48.05, 42.24, 36.37, 30.41, 29.43, 29.02, 27.21, 26.56, 24.76, 22.21, 20.95, 20.91, 20.82, 20.76 ppm. IR (neat): 1746, 1673 (cm^{-1}). MS (ESI) average m/z calcd for $C_{200}H_{333}N_{40}O_{64}$ $[M+5H]^{5+}$ 863.8801; found 863.8805.

Cluster 6c: Compound **6c** was obtained as a colorless oil in quantitative yield (42 mg, 12 μmol) from its acetylated precursor **31c** (52 mg, 12 μmol) according to the general procedure. $[\alpha]_D^{20} = -5.0$ ($c = 1.8$, CH_3OH). ^{1}H-NMR (MeOD, 500 MHz): δ 8.18–7.96 (br s, 4H, H-26), 7.95 (s, 4H, H-16), 4.77–3.93 (m, 56H, H-18, H-15, H-25, H-28 and H-30), 3.90-3.81 (m, 16H, H-6 and H-24), 3.73-3.17 (m, 96H, H-2, H-4, H-19, H-21 to H-23, H-31, H-32 and OCH_3), 3.13 (t, $J =$

9.3 Hz, 4H, H-3), 2.98 (dd, J = 11.0, 4.5 Hz, 4H, H-1a), 2.81–2.75 (m, 4H, H-7a), 2.58–2.53 (m, 4H, H-7b), 2.16 (t, J = 11.0 Hz, 4H, H-1b), 2.10 (dt, J = 9.5, 2.6 Hz, 4H, H-5), 1.93–1.87 (m, 8H, H-14), 1.50–1.44 (m, 8H, H-8), 1.31 (s, 40H, H-9 to H-13), 0.85 (s, 24H, CH_3) ppm. ^{13}C-NMR (MeOD, 125 MHz): δ 171.50, 146.24, 144.55, 125.50, 124.87, 80.60, 78.17, 77.33, 72.08, 72.02, 71.40, 70.78, 70.43, 67.37, 65.27, 59.55, 59.46, 59.41, 59.11, 57.75, 53.76, 51.50, 51.30, 43.35, 37.19, 31.29, 30.49, 29.98, 28.56, 27.43, 25.21, 22.64 ppm. IR (neat): 3400, 1668 (cm^{-1}). MS (ESI) average m/z calcd for $C_{168}H_{300}N_{40}O_{48}$ $[M+4H]^{4+}$ 911.5560; found 911.5587.

Acetylated cluster 32: Acetylated compound **32** (27 mg, 9.5 μmol, 64%) was prepared as a colorless oil according to the general procedure, starting from cyclopeptoid **8** (20 mg, 14.9 μmol) and ligand **15** (33.7 mg, 44.7 μmol). R_f = 0.33 (DCM/MeOH 9:1). $[\alpha]_D^{20}$ = + 0.5 (c = 0.8, $CHCl_3$). ^{1}H-NMR ($CDCl_3$, 400 MHz): δ 8.03–7.61 (br s, 2H, H-26), 7.49 (s, 2H, H-16), 5.09–5.00 (m, 4H, H-3 and H-4), 4.98–4.92 (m, 2H, H-2), 4.79–3.75 (m, 48H, H-18, H-28, H-15, H-25, H-30, H-6 and H-24), 3.72–2.95 (m, 88H, H-19, H-21 to H-23, H-31 to H-32, H-1a and OCH_3), 2.75–2.68 (m, 2H, H-7a), 2.62 (d, J = 8.0 Hz, 2H, H-5), 2.57–2.50 (m, 2H, H-7b), 2.31 (t, J = 10.8 Hz, 2H, H-1b), 2.06 (s, 6H, C(O)CH_3), 2.01 (s, 12H, C(O)CH_3), 2.00 (s, 6H, C(O)CH_3), 1.91–1.85 (m, 4H, H-14), 1.45-1.19 (m, 24H, H-8 to H-13), 0.86 (s, 12H, CH_3) ppm. ^{13}C-NMR ($CDCl_3$, 125 MHz): δ 171.04, 170.48, 170.15, 169.86, 169.11, 145.81, 143.64, 124.27, 122.15, 74.82, 71.49, 71.10, 70.61, 70.19, 69.64, 69.56, 65.21, 61.56, 59.63, 59.13, 58.84, 53.04, 51.88, 50.42, 48.16, 42.62, 36.41, 30.45, 29.48, 29.07, 27.26, 26.62, 24.79, 22.26, 21.00, 20.96, 20.87, 20.81 ppm. IR (neat): 1747, 1673 (cm^{-1}). MS (ESI) average m/z calcd for $C_{130}H_{218}KN_{26}NaO_{44}$ $[M+K+Na]^{2+}$ 1454.7572; found 1454.7581.

Cluster 7: Compound **7** was obtained as a colorless oil in quantitative yield (23 mg, 9.1 μmol) from its acetylated precursor **32** (26 mg, 9.1 μmol) according to the general procedure. $[\alpha]_D^{20}$ = −5.0 (c = 0.8, CH_3OH). ^{1}H-NMR (MeOD, 500 MHz): δ 8.17–7.96 (br s, 2H, H-26), 7.95 (s, 2H, H-16), 4.75–3.62 (m, 48H, H-18, H-15, H-25, H-28, H-30, H-6 and H-24), 3.59–3.16 (m, 90H, H-2, H-4, H-19, H-21 to H-23, H-31, H-32 and OCH_3), 3.13 (t, J = 9.0 Hz, 2H, H-3), 2.97 (dd, J = 11.0, 5.0 Hz, 2H, H-1a), 2.81–2.75 (m, 2H, H-7a), 2.58–2.53 (m, 2H, H-7b), 2.16 (t, J = 11.0 Hz, 2H, H-1b), 2.10 (dt, J = 9.5, 2.5 Hz, 2H, H-5), 1.92–1.86 (m, 4H, H-14), 1.51–1.45 (m, 4H, H-8), 1.32–1.29 (m, 20H, H-9 to H-13), 0.86 (s, 12H, CH_3) ppm. ^{13}C-NMR (MeOD, 125 MHz): δ 170.98, 161.46, 146.26, 144.48, 125.64, 124.88, 80.61, 78.18, 77.34, 72.11, 72.03, 71.42, 70.79, 70.42, 67.39, 65.25, 59.56, 59.40, 59.08, 57.75, 53.77, 51.52, 51.31, 43.46, 37.19, 31.30, 30.51, 30.49, 29.99, 28.57, 27.44, 25.22, 22.62 ppm. IR (neat): 3422, 1667 (cm^{-1}). MS (ESI) average m/z calcd for $C_{114}H_{204}N_{26}O_{36}$ $[M+2H]^{2+}$ 1256.7460; found 1256.7464.

General procedure for inhibition assay. The *p*-nitrophenyl-α-D-mannopyranoside and α-mannosidase (EC 3.2.1.24, from Jack Bean, K_m = 2.0 mM pH 5.5) were purchased from Sigma Aldrich. The release of *p*-nitrophenol was measured at 405 nm to determine initial velocities after basic quench with 1 M Na_2CO_3. All kinetics were performed between 23–25 °C and started by enzyme addition in a 100 μL assay medium (acetate buffer, 0.2 M, pH = 5.5 or 4) containing α-mannosidase (72 or 144 mU per mL), substrate (varying concentration from K_m/8 to 2K_m value) in presence or absence of various concentrations of inhibitor. K_i values were determined in triplicate, using the LB graphical method or non-linear regression. The inhibitors were dissolved in DMSO for concentrated mother solutions and DMSO/buffer for diluted solutions with a final DMSO concentration under 2.5% in all vials. Previously, the stability of the enzyme in presence of various concentrations of DMSO had been controlled and the enzyme activity was unaffected.

Analytical ultracentrifugation sedimentation velocity (**AUC–SV**) **experiments**. AUC-SV experiment and analysis were performed as described for cluster **1**[13] for the five compounds **3**, **4**, **5c**, **6c** and **7**.

Acknowledgements

The authors acknowledge financial support from the University of Strasbourg, the CNRS (LIMA-UMR 7042) and the Fondation Jean-Marie Lehn. Y. L. is grateful to the China Scholarship Council (CSC) for a PhD fellowship. The authors thank Dr. Emeric Wasielewski, responsible for the NMR research platform of LIMA (UMR7042 CNRS/Unistra) who contributed, by his valuable technical support, to the achievement of this work. The authors warmly acknowledge Catherine Birck for AUSV measurements and Alexandra Cousido-Siah for sample preparation. The computational part of this work was supported by research grants g2023a142c/g and g2022a262c/g from the Computer Center of the University of Strasbourg (CCUS). Financial support from the University of Salerno (FARB), from PRIN 2020: "Natural Products-Assisted Organic Synthesis" (2020AEX4TA) and from PRIN 2022 "CyPDRUGS: Cyclic peptoids in drug discovery: antimicrobial, antitumor and immunomodulating candidates" (P2022ZBNC2).

Conflict of Interests

The authors declare no conflict of interest.

Data Availability Statement

The data that support the findings of this study are available in the Supporting Information of this article.

Keywords: atomistic simulations · glycosidase · iminosugar · multivalency · thermodynamic modeling

[1] a) M. Mammen, S.-K. Choi, G. M. Whitesides, *Angew. Chem. Int. Ed.* **1998**, *37*, 2754–2794; b) C. Fasting, C. A. Schalley, M. Weber, O. Seitz, S. Hecht, B. Koksch, J. Dernedde, C. Graf, E.-W. Knapp, R. Haag, *Angew. Chem. Int. Ed.* **2012**, *51*, 10472–10498; c) S.-K. Choi, *Synthetic Multivalent Molecules: Concepts and Biomedical Applications*, Wiley, New York, **2004**.
[2] a) S. Cecioni, A. Imberty, S. Vidal, *Chem. Rev.* **2015**, *115*, 525–561; b) S. B. Yeldell, O. Seitz, *Chem. Soc. Rev.* **2020**, *49*, 6848–6865; c) M. González-Cuesta, C. Ortiz Mellet, J. M. García Fernández, *Chem. Commun.* **2020**, *56*, 5207–5222; d) C. Müller, G. Despras, T. K. Lindhorst, *Chem. Soc. Rev.* **2016**, *45*, 3275–3302; e) J. L. J. Blanco, C. Ortiz Mellet, J. M. G. Fernández, *Chem. Soc. Rev.* **2013**, *42*, 4518–4531; f) J. E. Gestwicki, C. W. Cairo, L. E. Strong, K. A. Oetjen, L. L. Kiessling, *J. Am. Chem. Soc.* **2002**, *124*, 14922–14933.
[3] Y. C. Lee, R. T. Lee, *Acc. Chem. Res.* **1995**, *28*, 321–327.
[4] a) C. R. Bertozzi, L. L. Kiessling, *Science* **2001**, *291*, 2357–2364; b) M. Martinez-Bailén, J. Rojo, J. Ramos-Soriano, *Chem. Soc. Rev.* **2023**, *52*, 536–572.
[5] For recent reviews see a) J. Ramos-Soriano, M. Ghirardello, M. C. Galan, *Chem. Soc. Rev.* **2022**, *51*, 9960–9985; b) M. Ogata, *Trends Glycosc. Glycotech.* **2021**, *33*, E91–E97; c) S. Leusmann, P. Ménová, E. Shanin, A. Titz, C. Rademacher, *Chem. Soc. Rev.* **2023**, *52*, 3663–3740.

[6] P. I. Kitov, J. M. Sadowska, G. Mulvey, G. D. Armstrong, H. Ling, N. S. Pannu, R. J. Read, D. R. Bundle, *Nature* **2000**, *403*, 669–672.
[7] a) M. L. Conte, S. Staderini, A. Chambery, N. Berthet, P. Dumy, O. Renaudet, A. Marra, A. Dondoni, *Org. Biomol. Chem.* **2012**, *10*, 3269–3277; b) A. Marra, S. Staderini, N. Berthet, P. Dumy, O. Renaudet, A. Dondoni, *Eur. J. Org. Chem.* **2013**, 1144–1149.
[8] P. Compain, C. Decroocq, J. Iehl, M. Holler, D. Hazelard, T. Mena Barragán, C. Ortiz Mellet, J.-F. Nierengarten, *Angew. Chem. Int. Ed.* **2010**, *49*, 5753–5756.
[9] For selected reviews see: a) P. Compain, A. Bodlenner, *ChemBioChem* **2014**, *15*, 1239–1251; b) S. G. Gouin, *Chem. Eur. J.* **2014**, *20*, 11616–11628; c) R. Zelli, J.-F. Longevial, P. Dumy, A. Marra, *New J. Chem.* **2015**, *39*, 5050–5074; d) C. Ortiz Mellet, J.-F. Nierengarten, J. M. G. Fernández, *J. Mater. Chem. B* **2017**, *5*, 6428–6436; e) P. Compain, *Chem. Rec.* **2020**, *20*, 10–22; f) Y. Wang, J. Xiao, A. Meng, C. Liu, *Molecules* **2022**, *27*, 5420.
[10] a) R. J. Pieters, *Org. Biomol. Chem.* **2009**, *7*, 2013–2025; b) V. Wittmann, R. J. Pieters, *Chem. Soc. Rev.* **2013**, *42*, 4492–4503.
[11] a) B. S. Gnanesh Kumar, G. Pohlentz, M. Schulte, M. Mormann, N. Siva Kumar, *Glycobiology* **2014**, *24*, 252–261; b) P. F. Daniel, B. Winchester, C. D. Warren, *Glycobiology* **1994**, *4*, 551–566; c) S. M. Snaith, *Biochem. J.* **1975**, *147*, 83–90.
[12] The first quantifiable multivalent effect in glycosidase inhibition (rp/n~2) was observed with JBα-man using di- to trivalent iminosugars: J. Diot, M. I. Garcia-Moreno, S. G. Gouin, C. Ortiz, Mellet, K. Haupt, J. Kovensky, *Org. Biomol. Chem.* **2009**, *7*, 357–363.
[13] M. L. Lepage, J. P. Schneider, A. Bodlenner, A. Meli, F. De Riccardis, M. Schmitt, C. Tarnus, N.-T. Nguyen-Huynh, Y.-N. Francois, E. Leize-Wagner, C. Birck, A. Cousido-Siah, A. Podjarny, I. Izzo, P. Compain, *Chem. Eur. J.* **2016**, *22*, 5151–5155.
[14] Polymeric inhibitors of bacterial sialidases based on transition-state analogues of sialyl substrates were recently reported to display relative inhibition potency up to four orders of magnitude on a valency corrected basis: C. Assailly, C. Bridot, A. Saumonneau, P. Lottin, B. Roubinet, E.-M. Krammer, F. François, F. Vena, L. Landemarre, D. Alvarez Dorta, D. Deniaud, C. Grandjean, C. Tellier, S. Pascual, V. Montembault, L. Fontaine, F. Daligault, J. Bouckaert, S. G. Gouin, *Chem. Eur. J.* **2021**, *27*, 3142–3150.
[15] E. Howard, A. Cousido-Siah, M. L. Lepage, J. P. Schneider, A. Bodlenner, A. Mitschler, A. Meli, I. Izzo, H. A. Alvarez, A. Podjarny, P. Compain, *Angew. Chem. Int. Ed.* **2018**, *57*, 8002–8006.
[16] E. V. Munoz, J. Correa, R. Riguera, E. Fernandez-Megia, *J. Am. Chem. Soc.* **2013**, *135*, 5966–5969.
[17] a) Y. Manabe, M. Tsutsui, K. Hirao, R. Kobayashi, H. Inaba, K. Matsuura, D. Yoshidome, K. Kabayama, K. Fukase, *Chem. Eur. J.* **2022**, *28*, e202201848; b) M. A. van Dongen, C. A. Dougherty, M. M. Banaszak Holl, *Biomacromolecules* **2014**, *15*, 3215–3234.
[18] V. Porkolab, M. Lepšík, S. Ordanini, A. S. John, A. L. Roy, M. Thépaut, E. Paci, C. Ebel, A. Bernardi, F. Fieschi, *ACS Cent. Sci.* **2023**, *9*, 709–718.
[19] E. J. Corey, *Angew. Chem. Int. Ed.* **1991**, *30*, 455–465.
[20] a) R. N. Zuckermann, J. M. Kerr, S. B. H. Kent, W. H. Moos, *J. Am. Chem. Soc.* **1992**, *114*, 10646–10647; b) G. Pierri, R. Schettini, F. F. Summa, F. De Riccardis, G. Monaco, I. Izzo, C. Tedesco, *Chem. Commun.* **2022**, *58*, 5253–5256; c) The synthesis of alkyne-functionalized core **8** was performed in the same way as for the other scaffolds by high dilution cyclization of linear precursor **8'** (see Figure S1 and ref. 20b).
[21] C. Decroocq, D. Rodríguez-Lucena, V. Russo, T. Mena Barragán, C. Ortiz Mellet, P. Compain, *Chem. Eur. J.* **2011**, *17*, 13825–13831.
[22] J. Jindrich, P. Kasal, Univerzita Karlova, Watrex Praha, WO-2021104547-A1, **2021**.
[23] M. M. Pichon, F. Stauffert, A. Bodlenner, P. Compain, *Org. Biomol. Chem.* **2019**, *17*, 5801–5817.
[24] A. Theil, J. Hitce, P. Retailleau, A. Marinetti, *Eur. J. Org. Chem.* **2006**, 154–161.
[25] M. Masuda, S. Miyazawa, Y. Ito, I. Matsuo, *J. Chin. Chem. Soc.* **2012**, *59*, 269–272.
[26] Z. Wang, Y. Gu, A. J. Zapata, G. B. Hammond, *J. Fluorine Chem.* **2001**, *107*, 127–132.
[27] B. C. Sanders, F. Friscourt, P. A. Ledin, N. E. Mbua, S. Arumugam, J. Guo, T. J. Boltje, V. V. Popik, G.-J. Boons, *J. Am. Chem. Soc.* **2011**, *133*, 949–957.
[28] N. Nebra, J. García-Álvarez, *Molecules* **2020**, *25*, 2015.
[29] J. F. Morrison, *Biochim. Biophys. Acta* **1969**, *185*, 269–286.
[30] S. Cha, *Biochem. Pharmacol.* **1975**, *24*, 2177–2185.
[31] Z. Aziz, M. A. Daugherty, J. G. de la Torre, B. Demeler, C. J. Douady, H. Durchschlag, K. G. Fleming, M. G. Fried, P. B. Furtado, H. E. Gilbert, *Analytical Ultracentrifugation: Techniques and Methods* Royal Society of Chemistry, **2007**, pp 1–23.
[32] J. Lebowitz, M. S. Lewis, P. Schuck, *Protein Sci.* **2002**, *11*, 2067–2079.
[33] P. Schuck, *Biophys. J.* **2010**, *98*, 2005–2013.
[34] G. J. Howlett, A. P. Minton, G. Rivas, *Curr. Opin. Chem. Biol.* **2006**, *10*, 430–436.
[35] S. Uchiyama, M. Noda, E. Krayukhina, *Biophys. Rev. Lett.* **2017**, *10*, 259–269.
[36] O. Boudker, O. SeCheol, *Methods* **2015**, *76*, 171–182.
[37] M. Spichty, Y. Liang, R. Schettini, I. Izzo, A. Bodlenner, P. Compain, *bioRxiv preprint* **2023**, DOI:10.1101/2023.11.29.569169.
[38] P. I. Kitov, D. R. Bundle, *J. Am. Chem. Soc.* **2003**, *125*, 16271–16284.
[39] B. Jönsson, M. Lund, F. L. Barroso da Silva, In *Food Colloids: Self-Assembly and Material Science, Vol. 302 (Eds: E. Dickinson, M. E. Leser)*, RSC Publishing, **2007**, pp. 129–154.
[40] For selected examples of iminosugar clusters designed as pharmacological chaperones for the treatment of lysosomal storage disorders see: a) C. Decroocq, D. Rodríguez-Lucena, K. Ikeda, N. Asano, P. Compain, *ChemBioChem* **2012**, *13*, 661–664; b) A. Joosten, C. Decroocq, J. de Sousa, J. Schneider, E. Etamé, A. Bodlenner, T. D. Butters, P. Compain, *ChemBioChem* **2014**, *15*, 309–319; c) G. D'Adamio, C. Matassini, C. Parmeggiani, S. Catarzi, A. Morrone, A. Goti, P. Paoli, F. Cardona, *RSC Adv.* **2016**, *6*, 64847–64851; d) S. Mirabella, G. D'Adamio, C. Matassini, A. Goti, S. Delgado, A. Gimeno, I. Robina, A. J. Moreno-Vargas, S. Šesták, J. Jiménez-Barbero, F. Cardona, *Chem. Eur. J.* **2017**, *23*, 14585–14596; e) M. L. Tran, M. Borie-Guichot, V. Garcia, A. Oukhrib, Y. Genisson, S. Ballereau, C. O. Turrin, C. Dehoux, *Chem. Eur. J.* **2023**, e202301210.

Manuscript received: December 11, 2023
Accepted manuscript online: January 15, 2024
Version of record online: February 13, 2024